


EUROPEAN UNION
European Structural and Investment Funds
Operational Programme Research,
Development and Education

FZU Institute of Physics of the Czech Academy of Sciences



# Optical spectroscopy and biosensors for investigation of biomolecules and their interactions

**Jakub Dostalek**

**AIT - Austrian Institute of Technology GmbH**
**Biosensor Technologies Unit**
Konrad-Lorenz-Strasse 24 | 3430 Tulln | Austria
T +43(0) 664 2351773

**FZU – Institute of Physics of the Czech Academy of Sciences**,
Na Slovance 1 | Prague 182 00 | Czech Republic
T+420 776767927

jakub.dostalek@ait.ac.at | http://www.ait.ac.at | http://www.jakubdostalek.cz

# Emerging Types of Optical Biosensors III – Sensors with Digital Readout

# Content

- General motivation for and increasing sensitivity in terms of LOD concentration
- Oligonucleotides - Digital PCR
- Proteins - Digital ELISA

# Motivation

EUROPEAN UNION
European Structural and Investment Funds
Operational Programme Research, Development and Education

MINISTRY OF EDUCATION, YOUTH AND SPORTS

FZU Institute of Physics of the Czech Academy of Sciences

AIT AUSTRIAN INSTITUTE OF TECHNOLOGY

# Concentration of Analytes in Clinical Samples

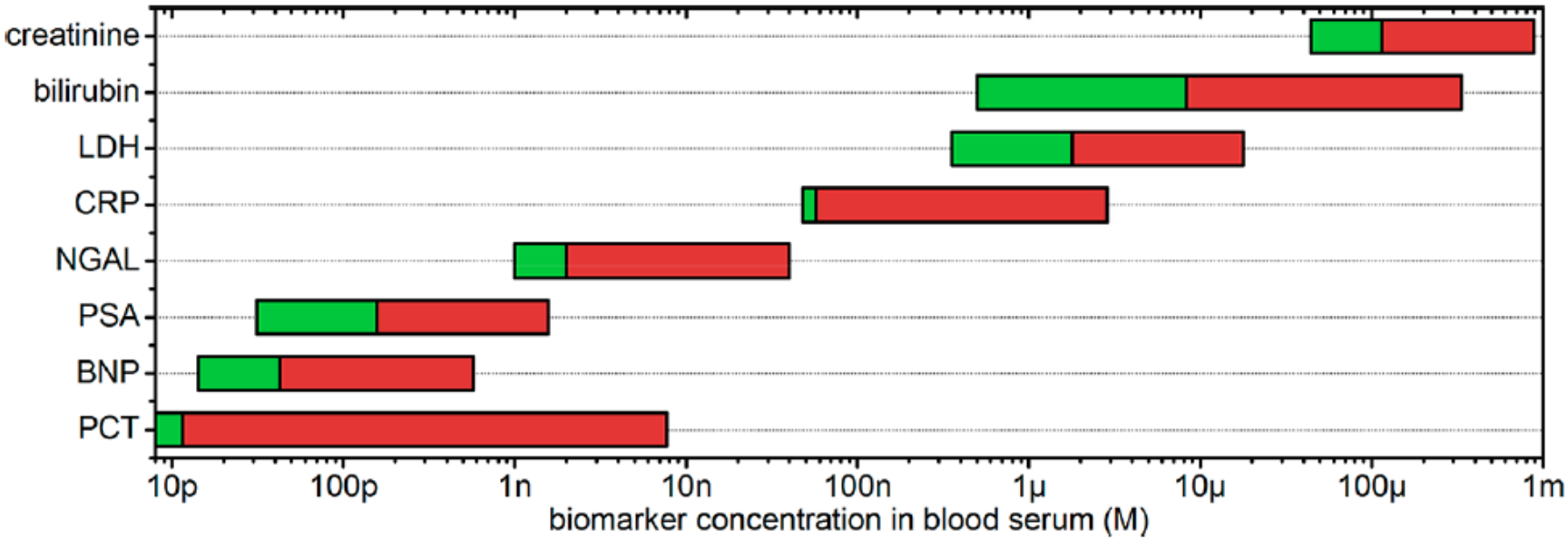


Typical concentration range of clinically relevant biomarkers in blood serum. The green bars indicate reference values for healthy persons, whereas the red extension to the right indicates elevated values associated with disease. LDH: lactate dehydrogenase, CRP: c-reactive protein, NGAL: neutrophil gelatinase-associated lipocalin, PSA: prostate specific antigen, BNP: B-type natriuretic peptide, PCT: pro-calcitonin

Mayo Medical Laboratories; www.mayomedicallaboratories.com, accessed 19-5-2017.

# Concentration of Analytes in Clinical Samples

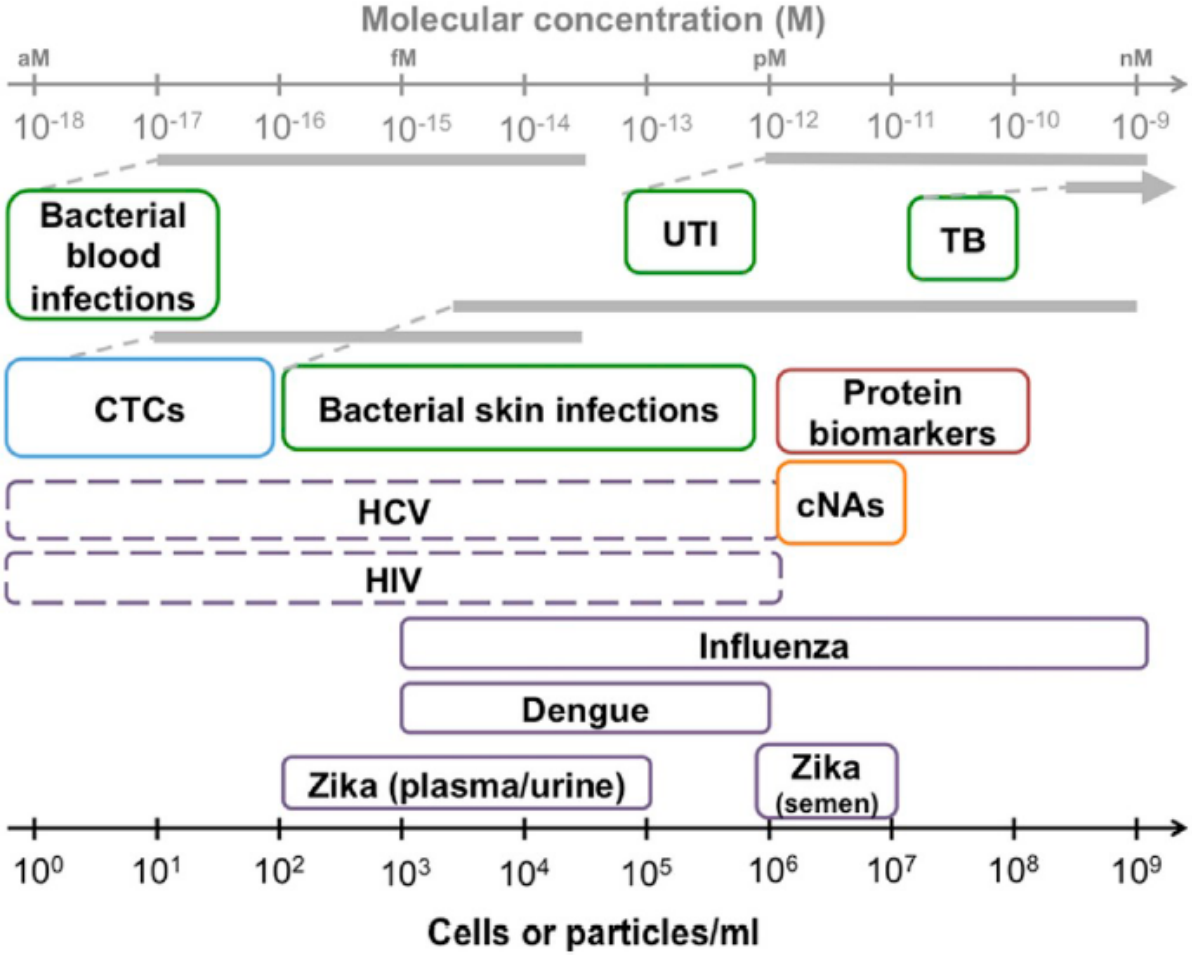


Kelley, S.O., 2017. What are clinically relevant levels of cellular and biomolecular analytes? ACS Sens. 2 (2), 193–197.

# Single Molecule Detection

- Ultimate sensitivity enabling counting of individual molecules

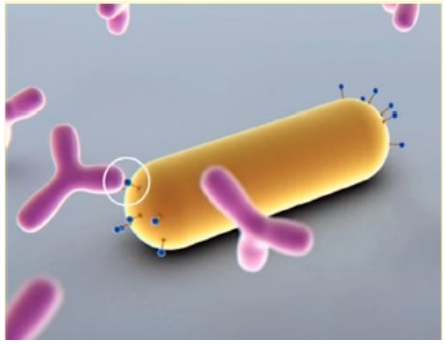

- Single molecule detection possible with miniature sensor transducers or by the detection in tightly confined volumes.
- Single molecule detection sensors typically operate high concentrations, and themselves do not provide ultrasensitive detection in terms of minute concentrations of target analyte on macroscopic volume of a liquid sample (tyranny of slow diffusion)
- Possible solution is compartmenting the sample volume to many smaller volume interfaces with individual sensors.

# Compartments

- $\lambda$ represents the average number of target molecules per one microcompartment

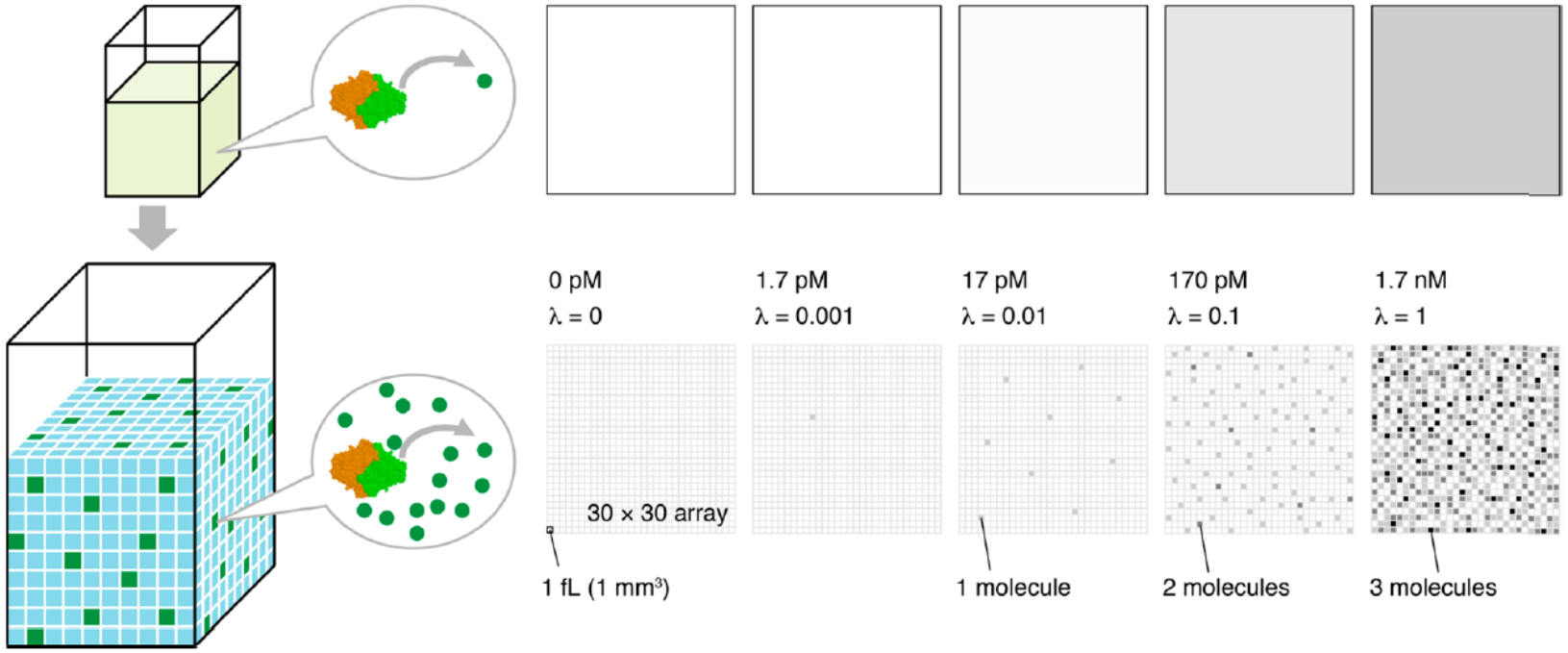


DOI: 10.1021/acs.analchem.6b04290

Concept of the digital bioassay. A schematic comparison between analog measurement and digital counting is shown. In digital bioassays (bottom part), the bulk reaction solution is partitioned into extremely small compartments to rapidly concentrate the reaction product. In conventional tube-based assays (top part), the reaction product diffuses very quickly, making a highly diluted product difficult to detect. The exemplary concentration is calculated on the basis of a microcompartment volume of 1 fL (corresponding to height, width, and depth of 1 µm).

# Statistics of Bionomial Trials

- The probability "P" of event A occurring k times among n molecules obeys a binomial distribution, which is denoted as X ~ B(n, p):

$$P(X = k) = \binom{n}{k} p^k (1 - p)^{(n-k)} \quad (k = 0, 1, 2, \ldots, n)$$

- The binomial distribution converges toward the Poisson distribution:

$$\lim_{n \to \infty, p \to 0} \binom{n}{k} p^k (1 - p)^{(n-k)} = e^{-\lambda} \frac{\lambda^k}{k!} \quad (\lambda = np,\ k = 0, 1, 2, \ldots, n)$$

$\lambda = n/m = c \cdot v \cdot \mathrm{NA}$
$p = 1/m$
$n$ – number of molecules in the whole volume
$m$ – number of compartments
$v$ – volme of compartments
$k$ – number of molecules in the compartment
$c$ - bulk molar concentration of the target molecule

10.1021/acs.analchem.6b04290

- For low concentrations, $P_{\text{positive}} = 1\text{-}P(X=0) = 1 - e^{-\lambda} \sim \lambda$

# Compartmentalization Methods

# Digital PCR - Overview of Volume

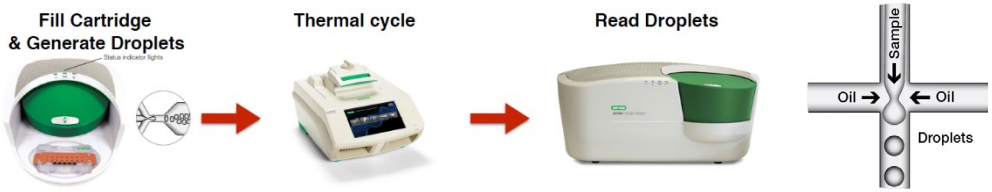


**BioRad**
Droplets

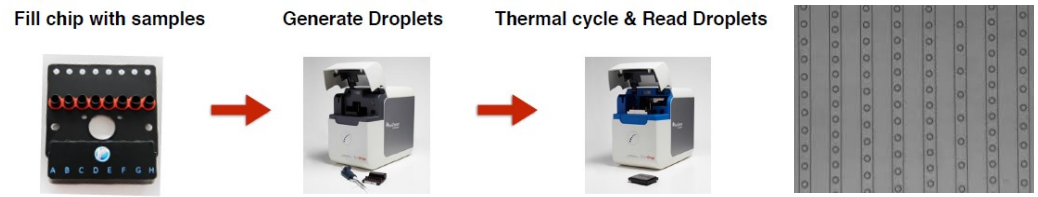


**Raindance**
Droplets

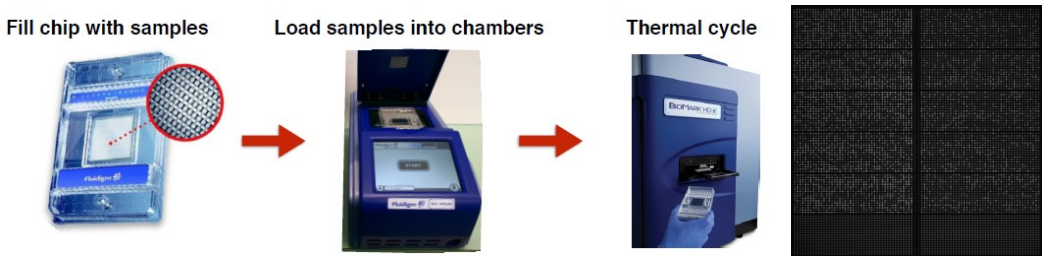


**Fluidigm**
Reaction chambers
6 nL

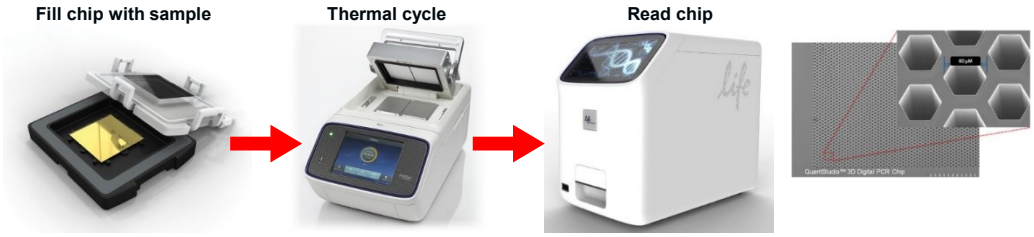


**Applied Biosystems**
Reaction wells
33 nL

EUROPEAN UNION
European Structural and Investment Funds
Operational Programme Research,
Development and Education

MINISTRY OF EDUCATION, YOUTH AND SPORTS

FZU Institute of Physics of the Czech Academy of Sciences

AIT AUSTRIAN INSTITUTE OF TECHNOLOGY

# Lithographically made Arrays of Wells

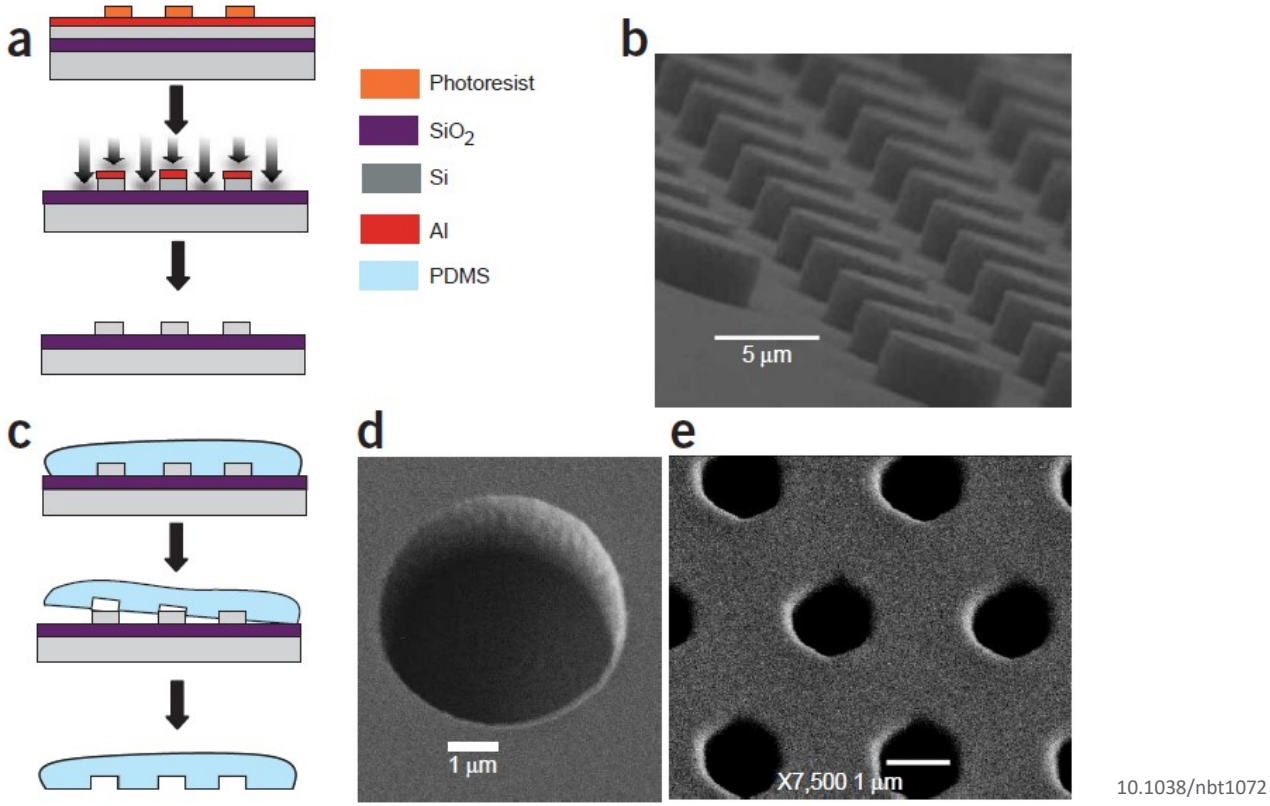


10.1038/nbt1072

- Prepared by using soft lithography from a mold with arrays of pillars. Transferred to a Teflon-based materials.

EUROPEAN UNION
European Structural and Investment Funds
Operational Programme Research,
Development and Education

MINISTRY OF EDUCATION, YOUTH AND SPORTS

FZU Institute of Physics of the Czech Academy of Sciences

AIT AUSTRIAN INSTITUTE OF TECHNOLOGY

# Microdroplet Generators

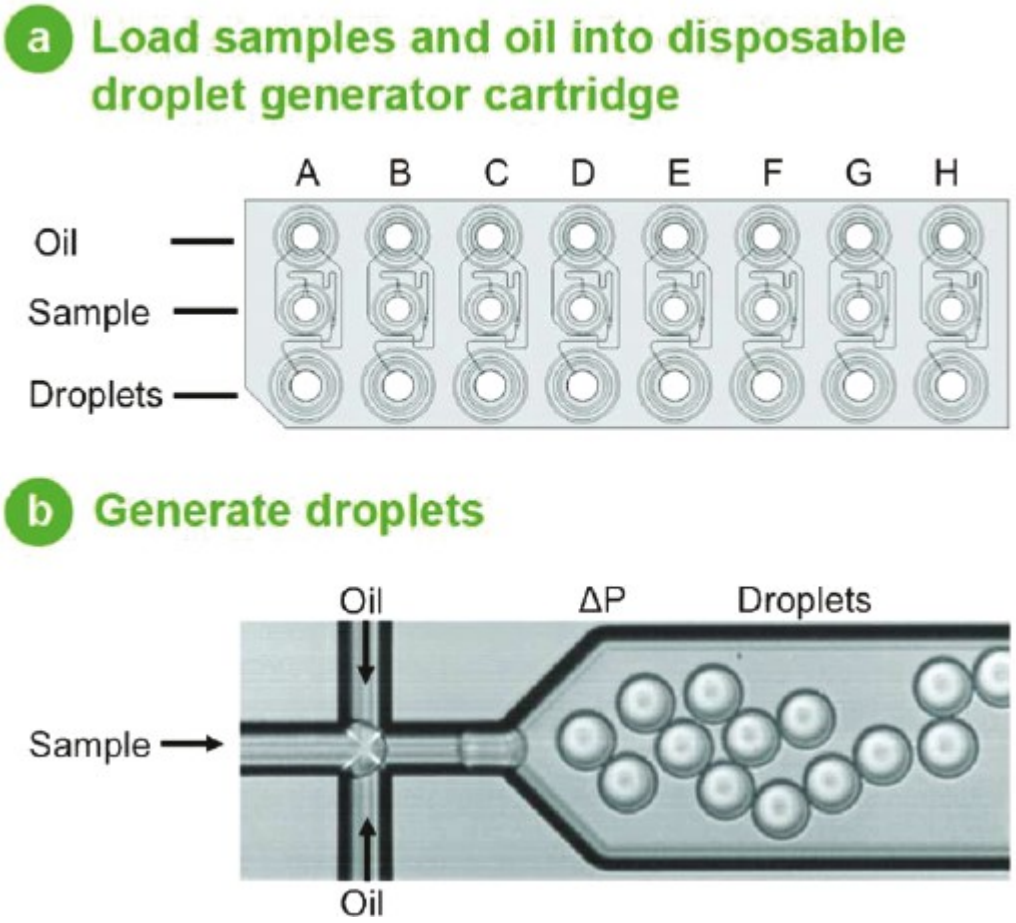


dx.doi.org/10.1021/ac202028g

EUROPEAN UNION
European Structural and Investment Funds
Operational Programme Research,
Development and Education

MINISTRY OF EDUCATION, YOUTH AND SPORTS

FZU Institute of Physics of the Czech Academy of Sciences

AIT AUSTRIAN INSTITUTE OF TECHNOLOGY

# Lithographically made Arrays of Wells

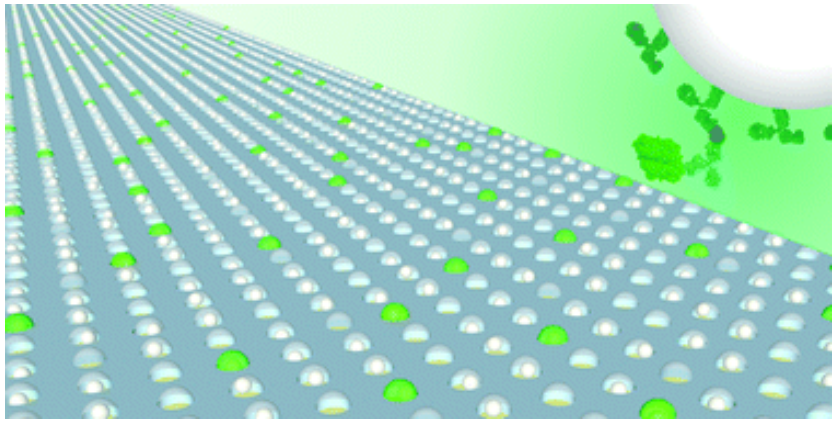

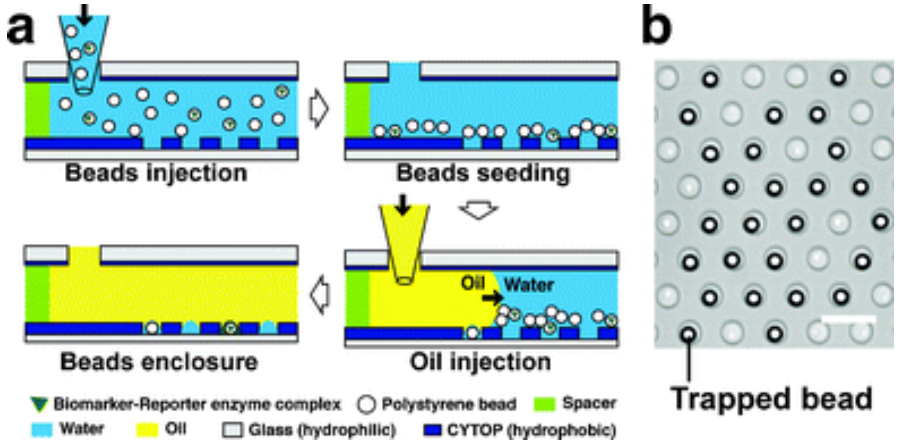


10.1039/C2LC40632B

- Arrays of wells with volume of fL (scale bar 10 micron) for trapping of magnetic beads carrying target analyte.

# Lithographically made Arrays of Wells

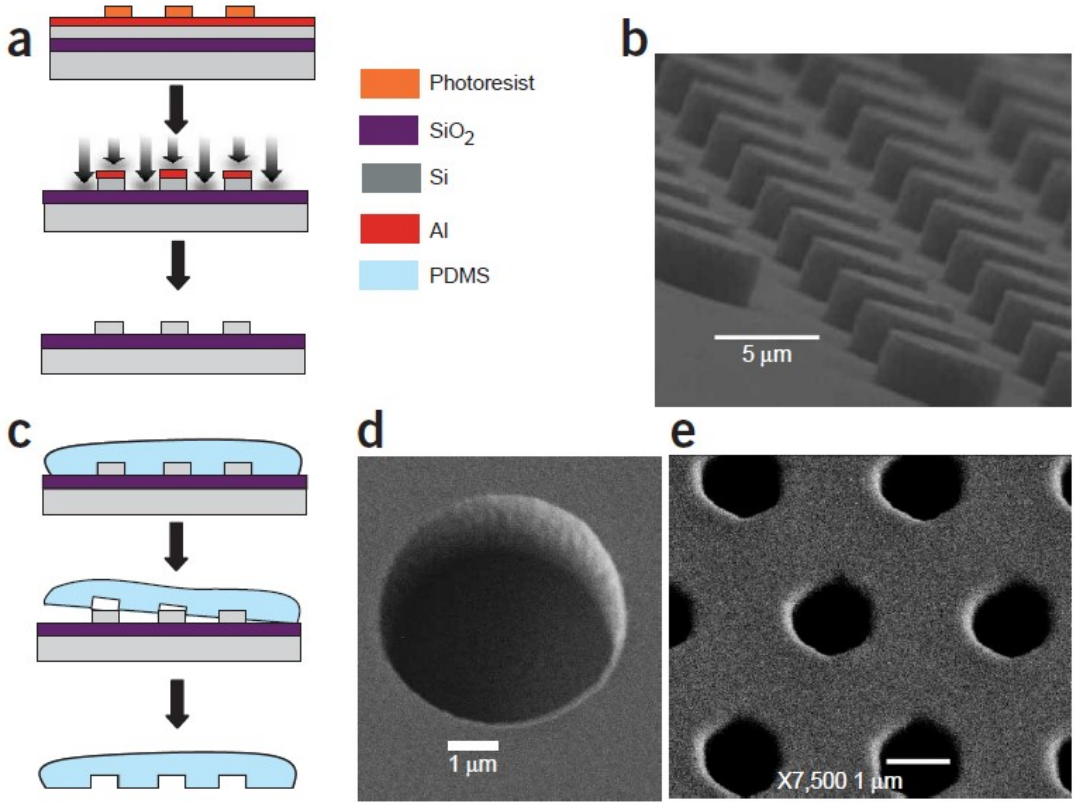


10.1038/nbt1072

- Prepared by using soft lithography from a mold with arrays of pillars. Transferred to a Teflon-based materials.

# Lithographically made Arrays of Wells

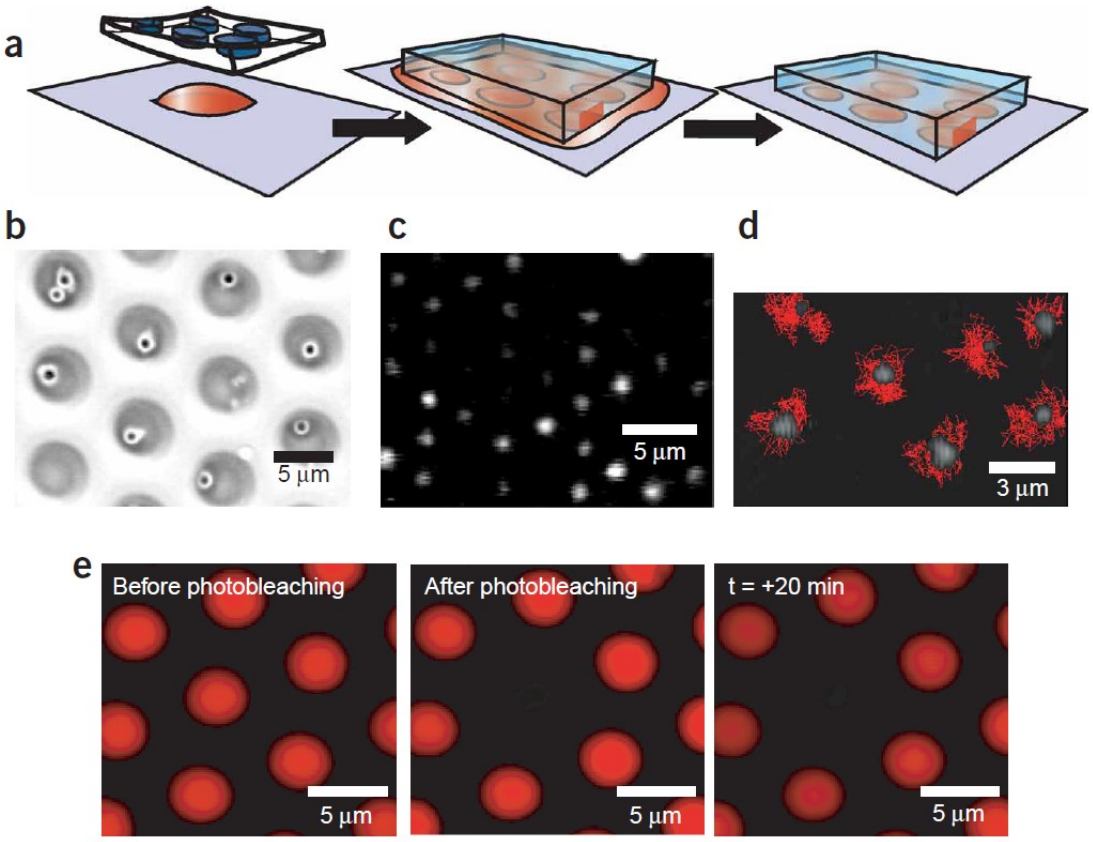


10.1038/nbt1072

- Testing of sealing of compartments by fluorescence tracking of individual molecules and photo-bleaching of emitters.

# Microemulsion

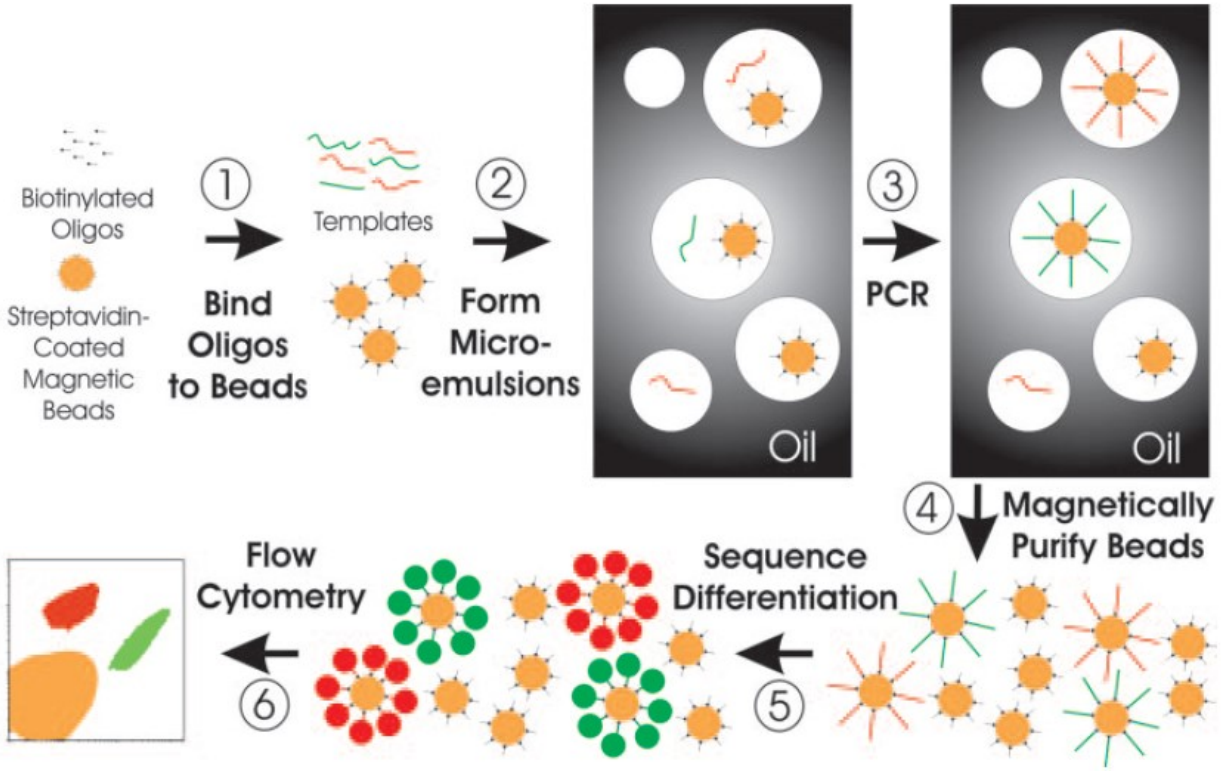


www.pnas.orgcgidoi10.1073pnas.1133470100

- Microemulsions – prepared by stirring a mixture of oil and aqueous phase (sort of mayonaisse?)

# Detection of Nucleic Acids

# Polymerase Chain Reaction - PCR

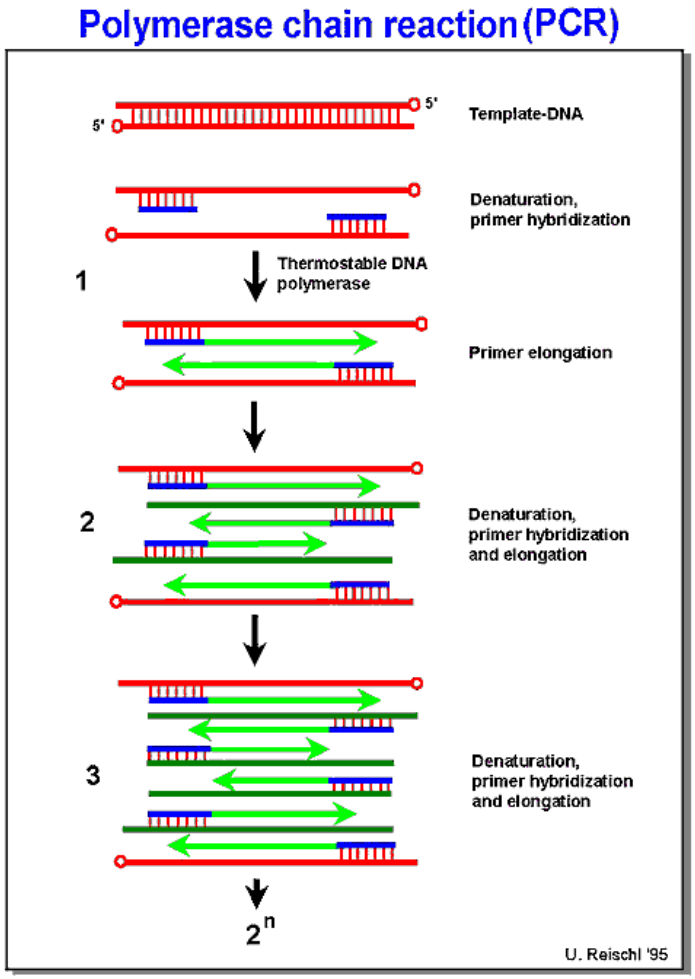


Thermocycling

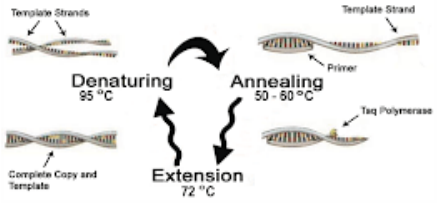


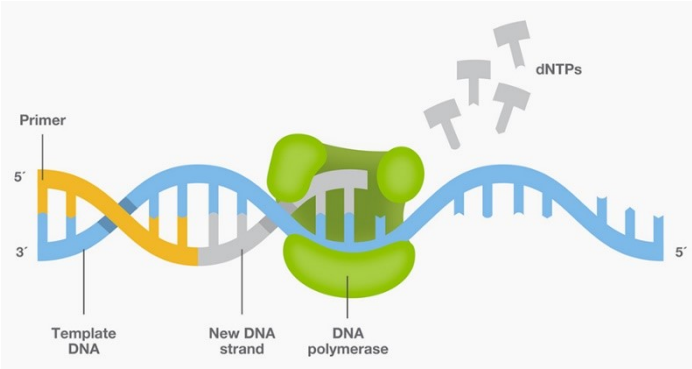


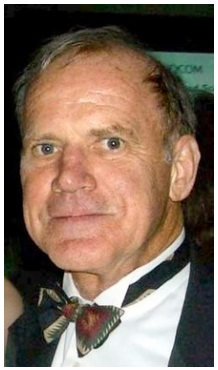

Karry Mullis was awarded the Nobel Prize in Chemistry in 1993 for inventing PCR

EUROPEAN UNION
European Structural and Investment Funds
Operational Programme Research, Development and Education

MINISTRY OF EDUCATION, YOUTH AND SPORTS

FZU Institute of Physics of the Czech Academy of Sciences

AIT AUSTRIAN INSTITUTE OF TECHNOLOGY

# Fluorescence Resonant Energy Transfer - FRET

**Förster / fluorescence resonant energy transfer: dipole-dipole coupling of two fluorophores which changes the emission spectrum. Efficient at small distances, typically $r < 10$ nm.**

$$E = \frac{1}{1 + (r/R_0)^6}$$

$R_0$ is Förster distance at which $E$=50%

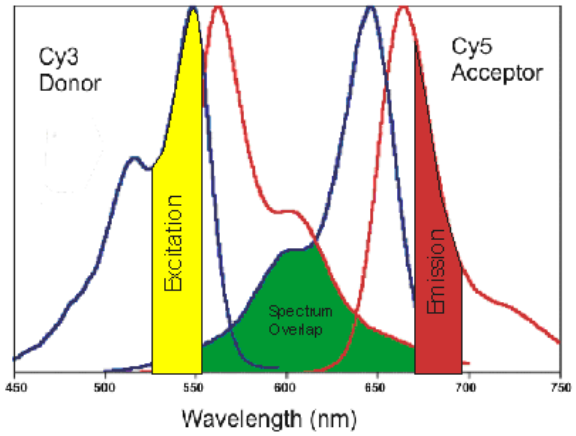


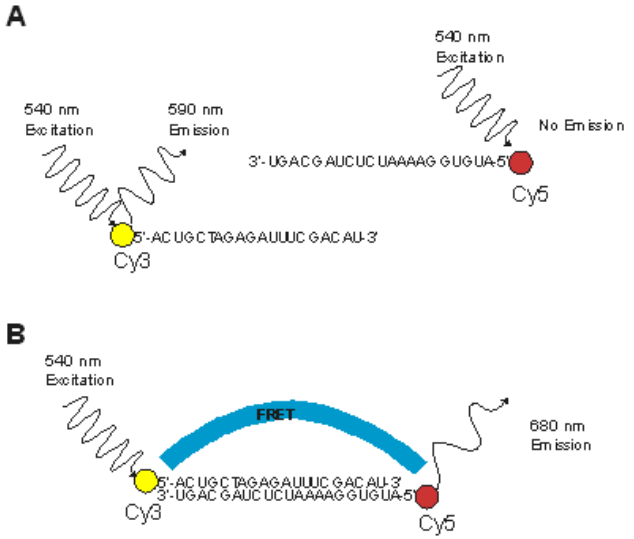


Spectral overlap of absoprtion and emission bands of donor and acceptor chromophores

Applications: conformation changes studies, immunoassays, DNA hybridization.

# Readout of the PCR Product

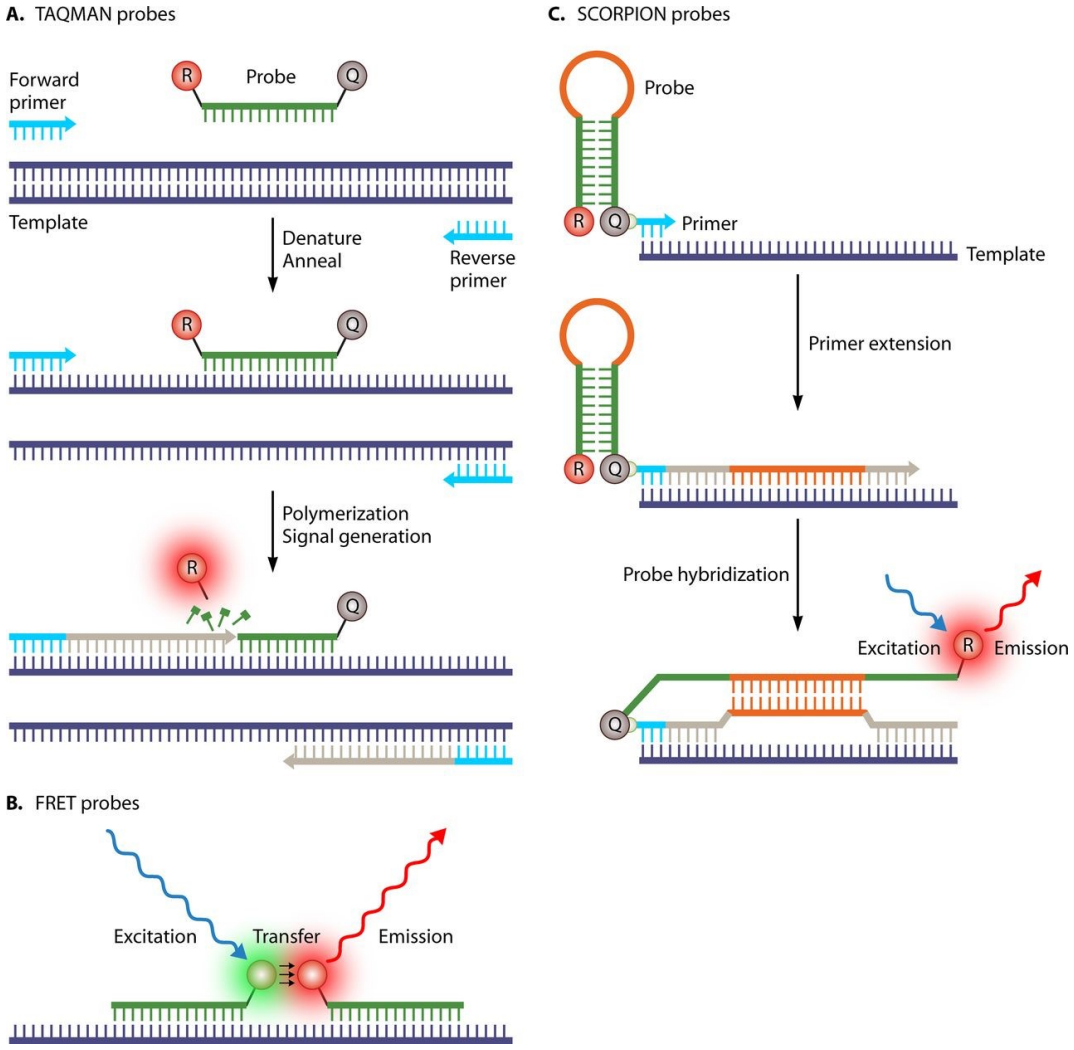


- Probes are loaded to a droplet together with sample and PCR reagents
- Without the analyte they are dark and when the target analyte is present, are turned to bright.
- Based on fluorescence and FRET or quenching.

EUROPEAN UNION
European Structural and Investment Funds
Operational Programme Research, Development and Education

MINISTRY OF EDUCATION, YOUTH AND SPORTS

FZU Institute of Physics of the Czech Academy of Sciences

AIT AUSTRIAN INSTITUTE OF TECHNOLOGY

# Digital PCR

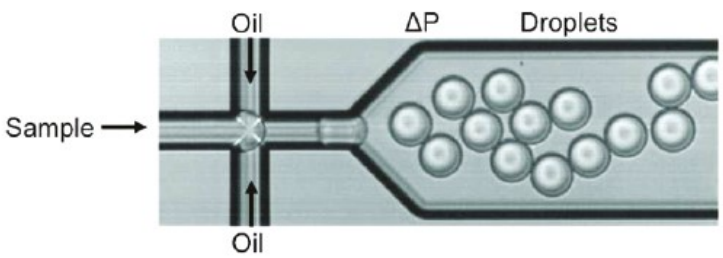


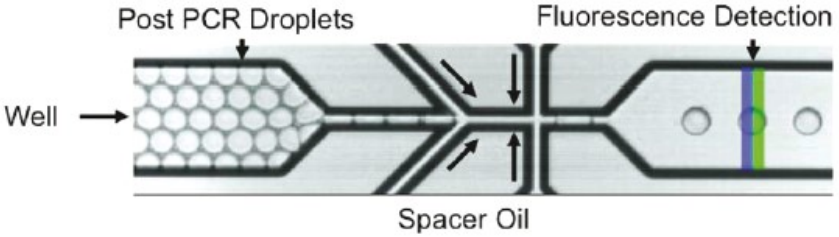


c Transfer droplets to 96-well PCR plate

d Thermal cycle to end-point

e Read droplet fluorescence

f Apply amplitude thresholds and calculate concentrations

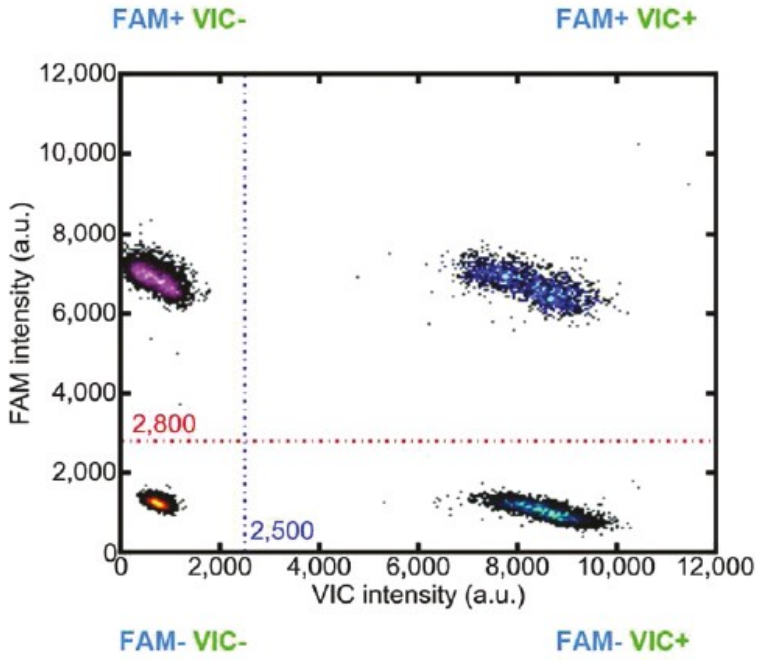


- Droplets are assigned as positive or negative based on their fluorescence amplitude. Calculated the concentration of the target and reference DNA sequences and their Poisson-based 95% confidence intervals.

dx.doi.org/10.1021/ac202028g

# Single DNA Molecule Sequencing

- Using zero-mode optical waveguides, light probing is confined to about 0.1 µm. Monitoring of assembly of individual nucleotides carrying specific fluorescent tags.

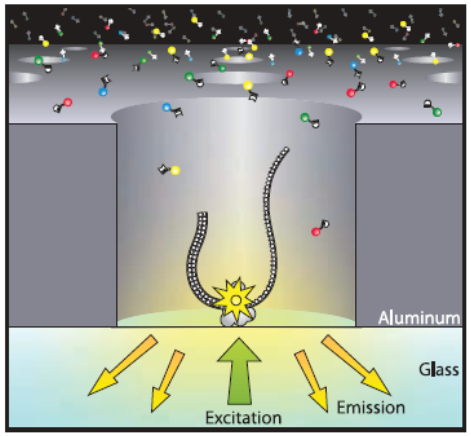


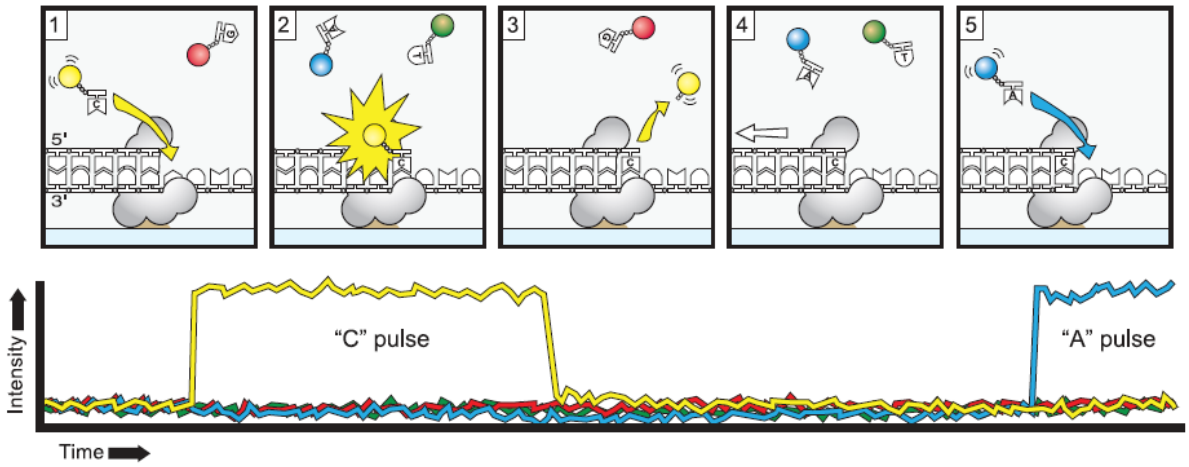


S. Real-Time DNA Sequencing from Single Polymerase Molecules. Science 2009, 323 (5910), 133–138.

# Single Molecule Interaction Analysis

- Labelling of bases with different dye molecules allows monitoring in real time assembly and prolongation of the duplex base by base.

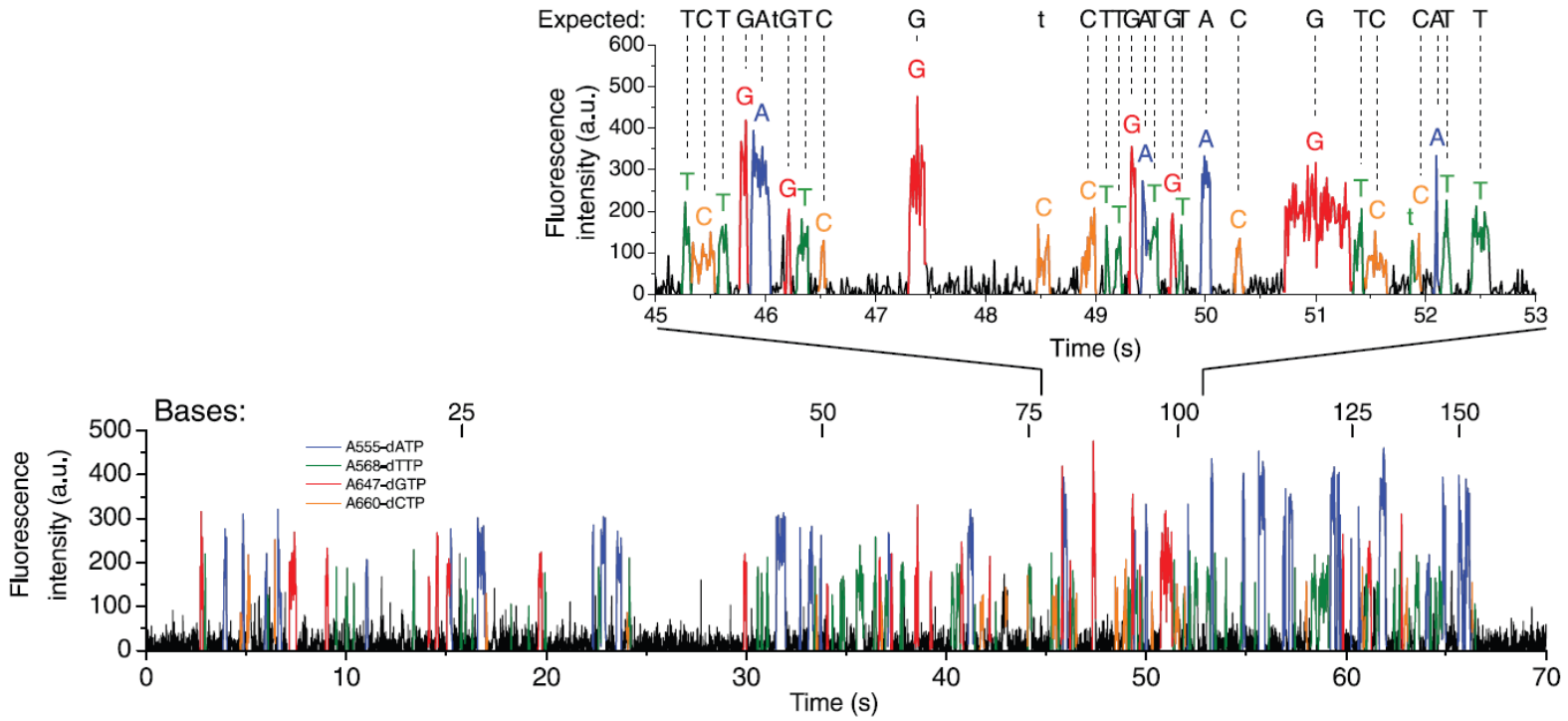


Pacific Biosciences: http://www.pacb.com/

S. Real-Time DNA Sequencing from Single Polymerase Molecules. Science 2009, 323 (5910), 133–138.

# Zero-Mode Waveguide

https://doi.org/10.1038/s41598-020-61856-9

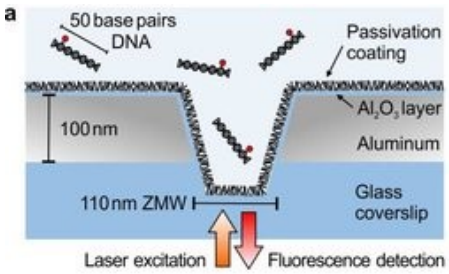


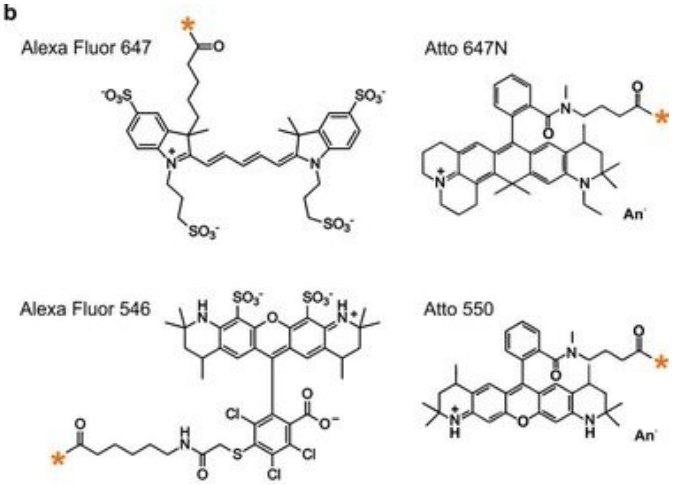


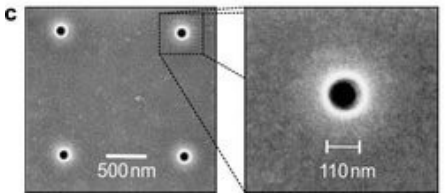


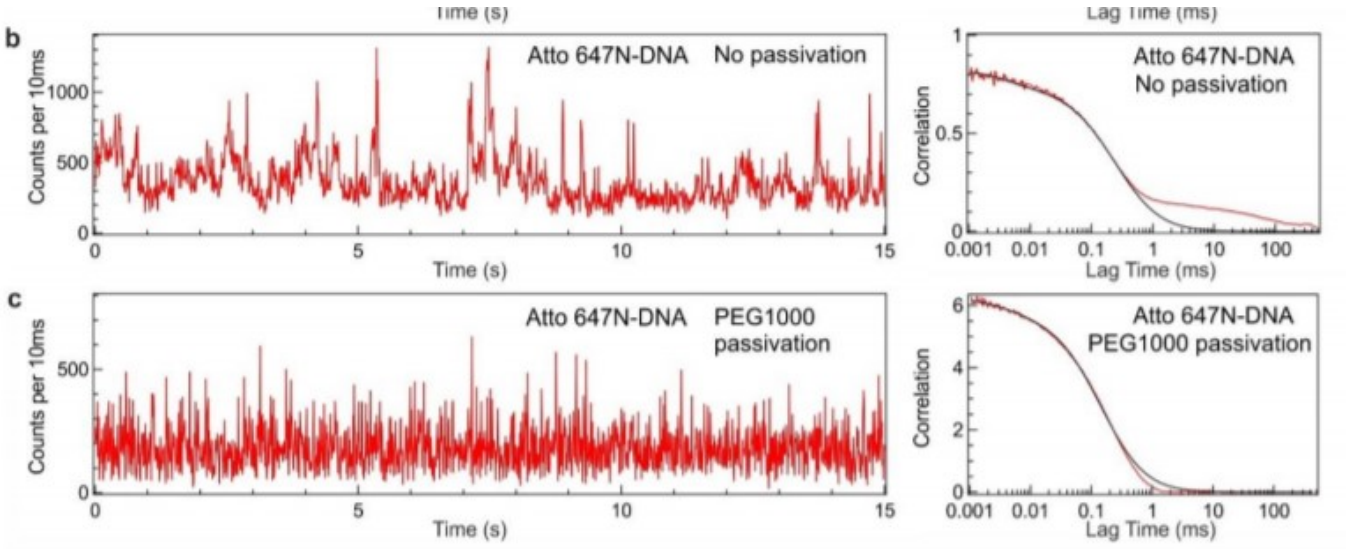

# Detection of Protein Analytes

EUROPEAN UNION
European Structural and Investment Funds
Operational Programme Research,
Development and Education

MINISTRY OF EDUCATION, YOUTH AND SPORTS

FZU Institute of Physics of the Czech Academy of Sciences

AIT AUSTRIAN INSTITUTE OF TECHNOLOGY

# Enzyme-Linked Immunosorbent Assays

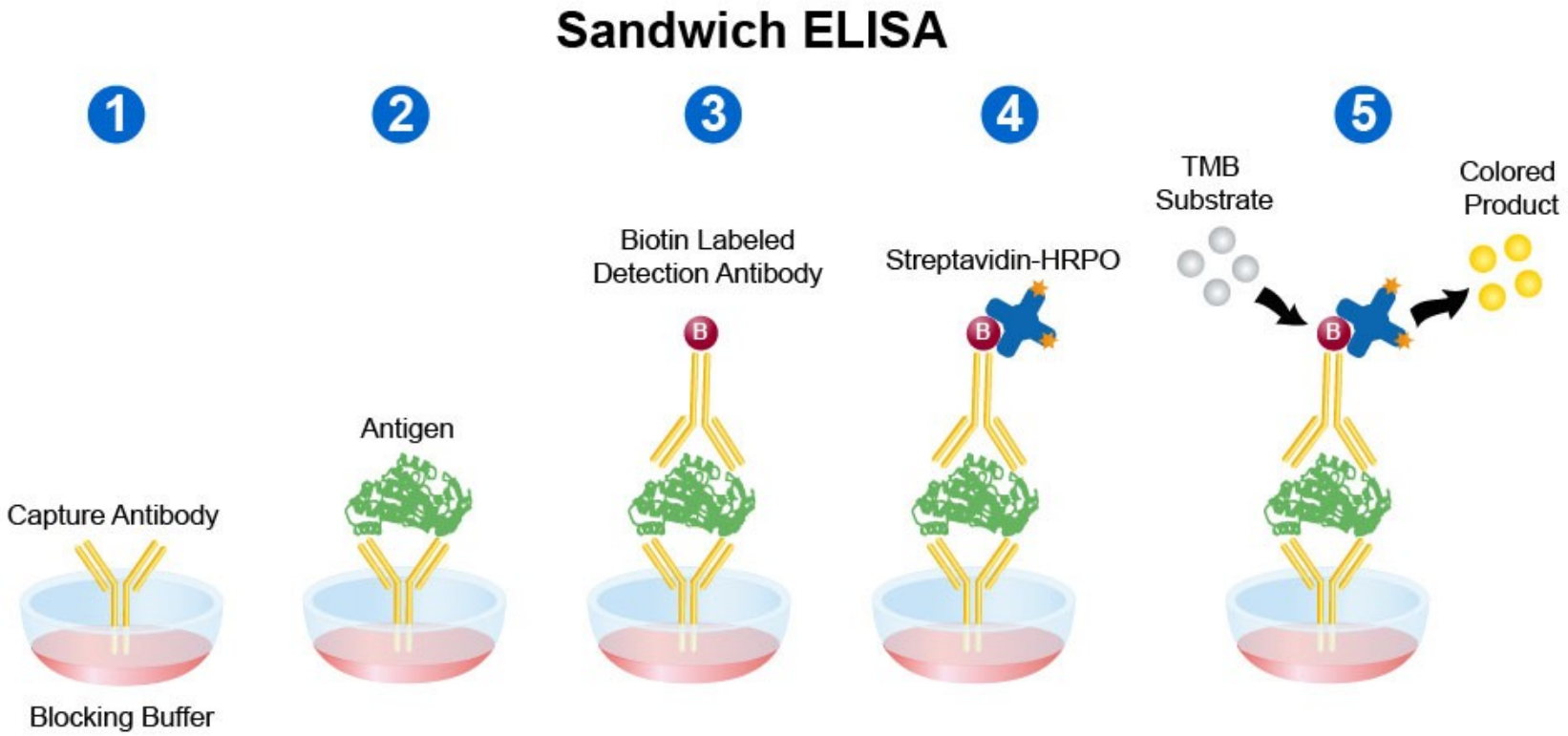


https://www.leinco.com/sandwich-elisa-protocol/

# Enzyme-linker Immunosorbent Assays

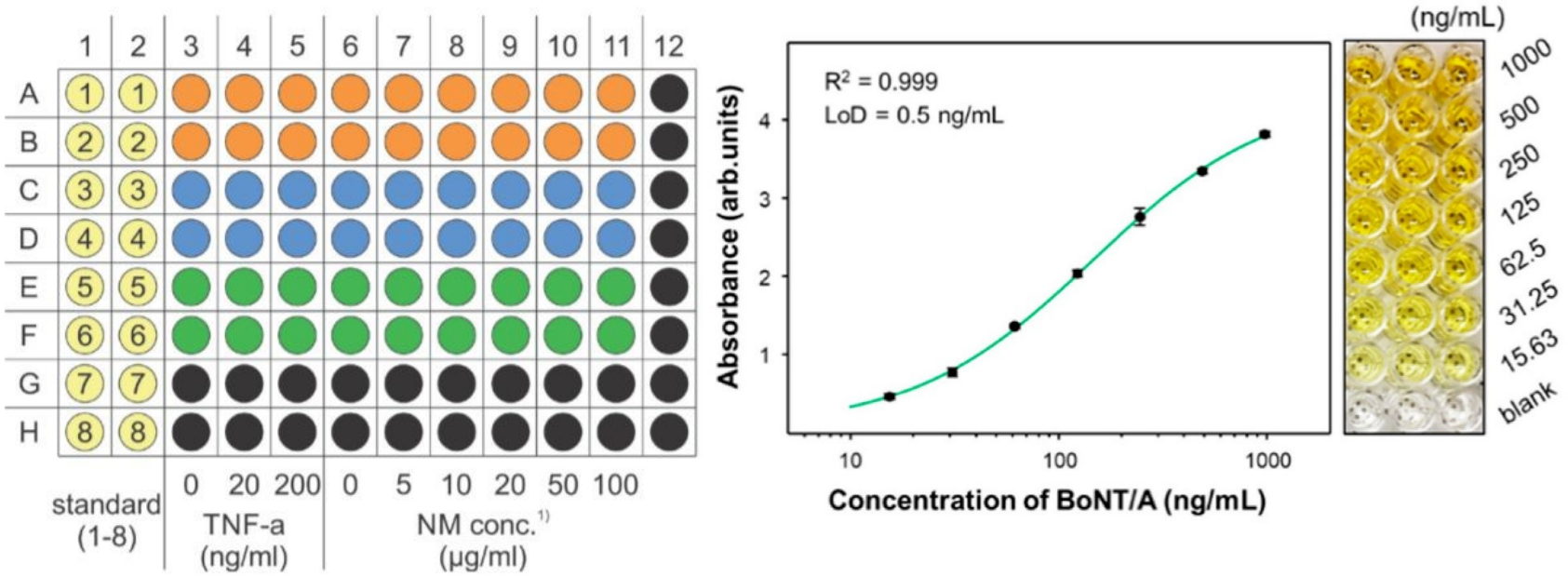


https://www.nanopartikel.info/files/methodik/VIGO/I_ELISA_A549.pdf

https://doi.org/10.3390/s19194081

- ELISA replaced radio-immunoassays in 1970ties, still routinely used and other enzymatic reactions exploited for faster and more sensitive readout.

EUROPEAN UNION
European Structural and Investment Funds
Operational Programme Research,
Development and Education

MINISTRY OF EDUCATION, YOUTH AND SPORTS

FZU Institute of Physics of the Czech Academy of Sciences

AIT AUSTRIAN INSTITUTE OF TECHNOLOGY

# Fluorescence – More Sensitive Readout

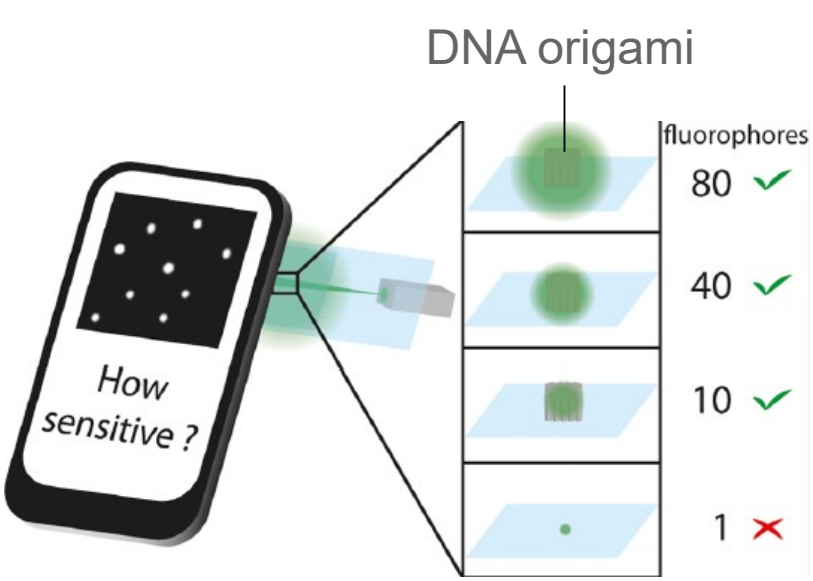


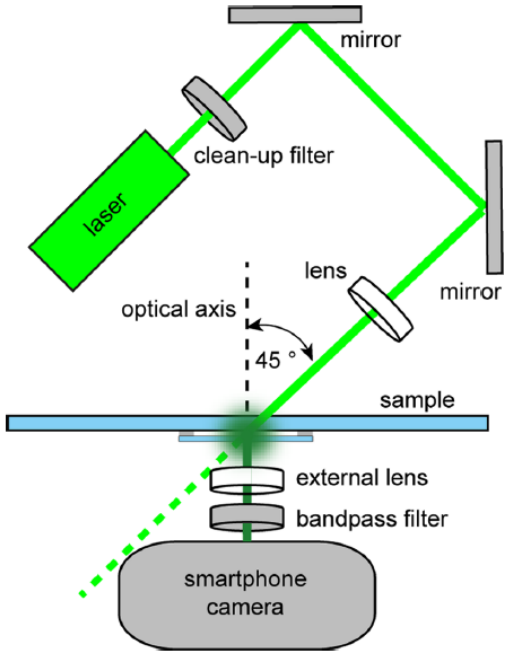


DOI: 10.1021/acsomega.8b03136
ACS Omega 2019, 4, 637−642

- Fluorescence readout can be implemented also with cheap optics, not only high end fluorescence microscopes.

EUROPEAN UNION
European Structural and Investment Funds
Operational Programme Research,
Development and Education

MINISTRY OF EDUCATION, YOUTH AND SPORTS

FZU Institute of Physics of the Czech Academy of Sciences

AIT AUSTRIAN INSTITUTE OF TECHNOLOGY

# Fluorescence Readout Comparison

DOI: 10.1021/acsomega.8b03136
ACS Omega 2019, 4, 637−642

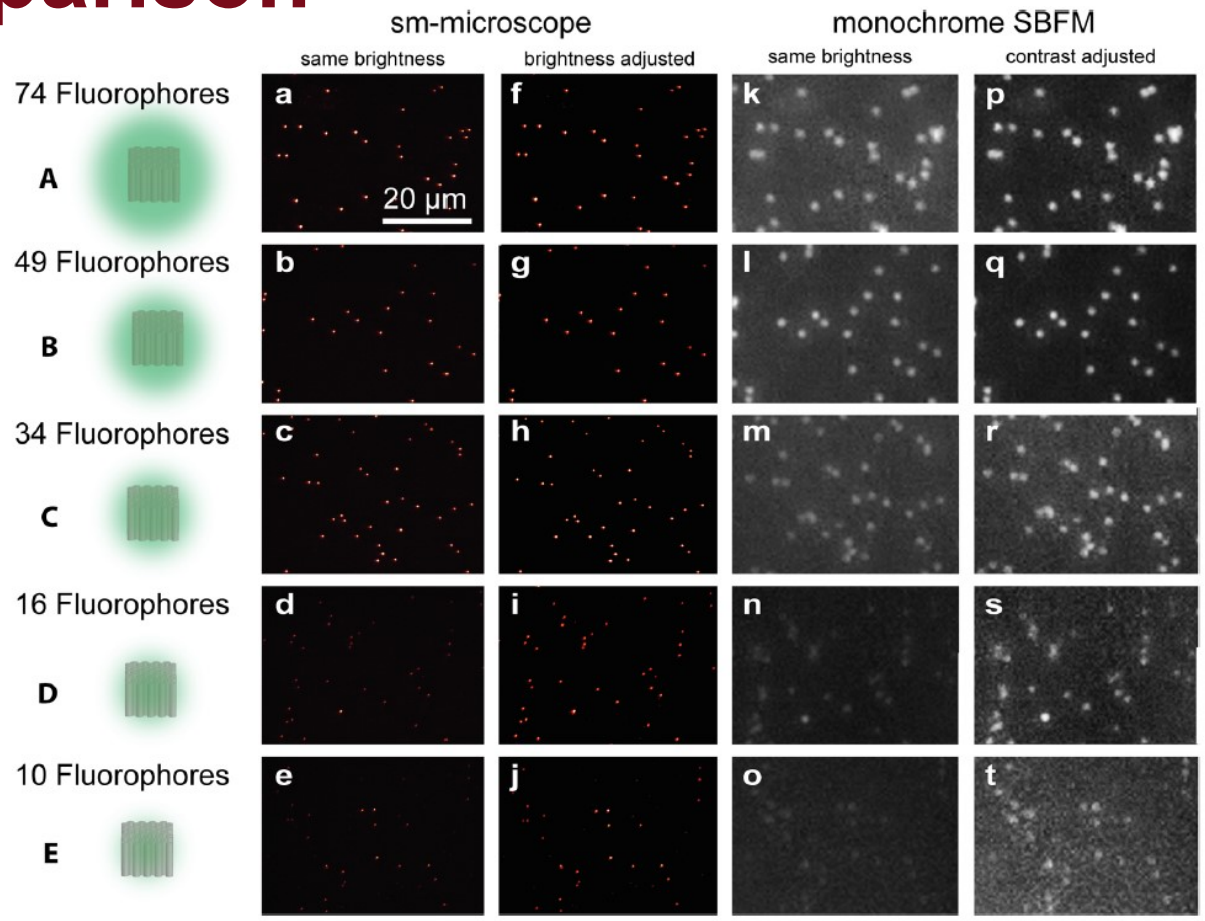

# Fluorescence-Based Probing

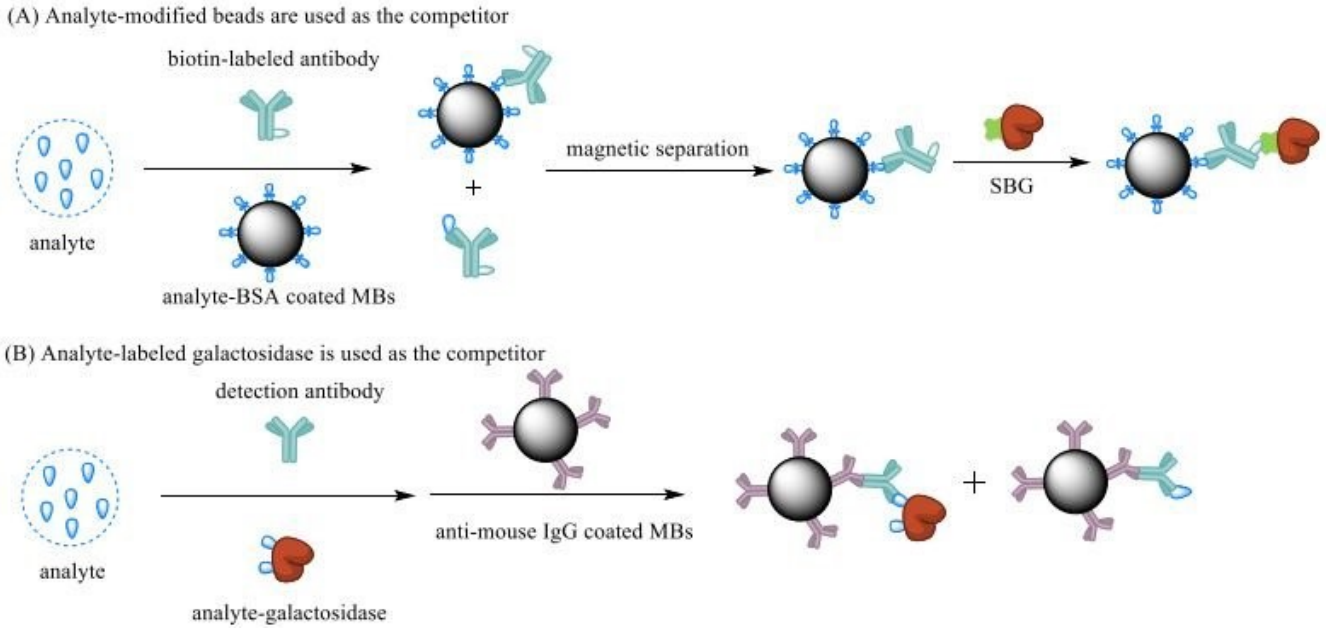


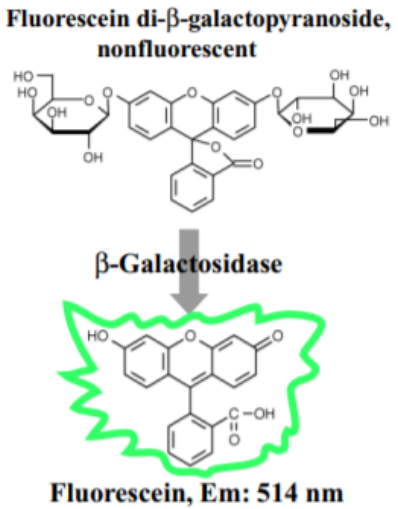


- Beta galactosidase hydrolyzes fluorescein-di-b-D-galactopyranoside to fluorescein.
- Beta galactosidase serves as a label in immunoassays.

doi:10.1038/nbt1072

EUROPEAN UNION
European Structural and Investment Funds
Operational Programme Research,
Development and Education

MINISTRY OF EDUCATION, YOUTH AND SPORTS

FZU Institute of Physics of the Czech Academy of Sciences

AIT AUSTRIAN INSTITUTE OF TECHNOLOGY

# Single Enzyme Detection

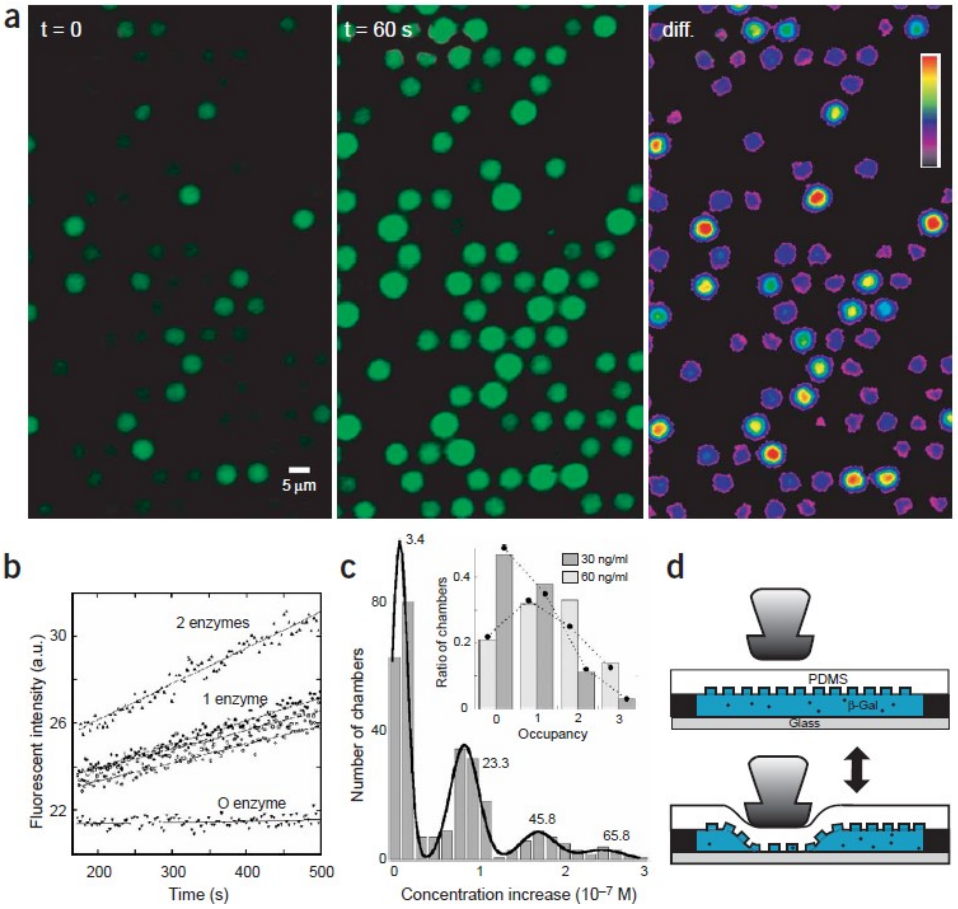


doi:10.1038/nbt1072

- Fluorescence-based detection in confined (30 fL) allowed for discriminating single beta galactosidase molecules.

EUROPEAN UNION
European Structural and Investment Funds
Operational Programme Research, Development and Education

MINISTRY OF EDUCATION, YOUTH AND SPORTS

FZU Institute of Physics of the Czech Academy of Sciences

AIT AUSTRIAN INSTITUTE OF TECHNOLOGY

# Digital ELISA

https://doi.org/10.1016/j.aca.2018.02.011

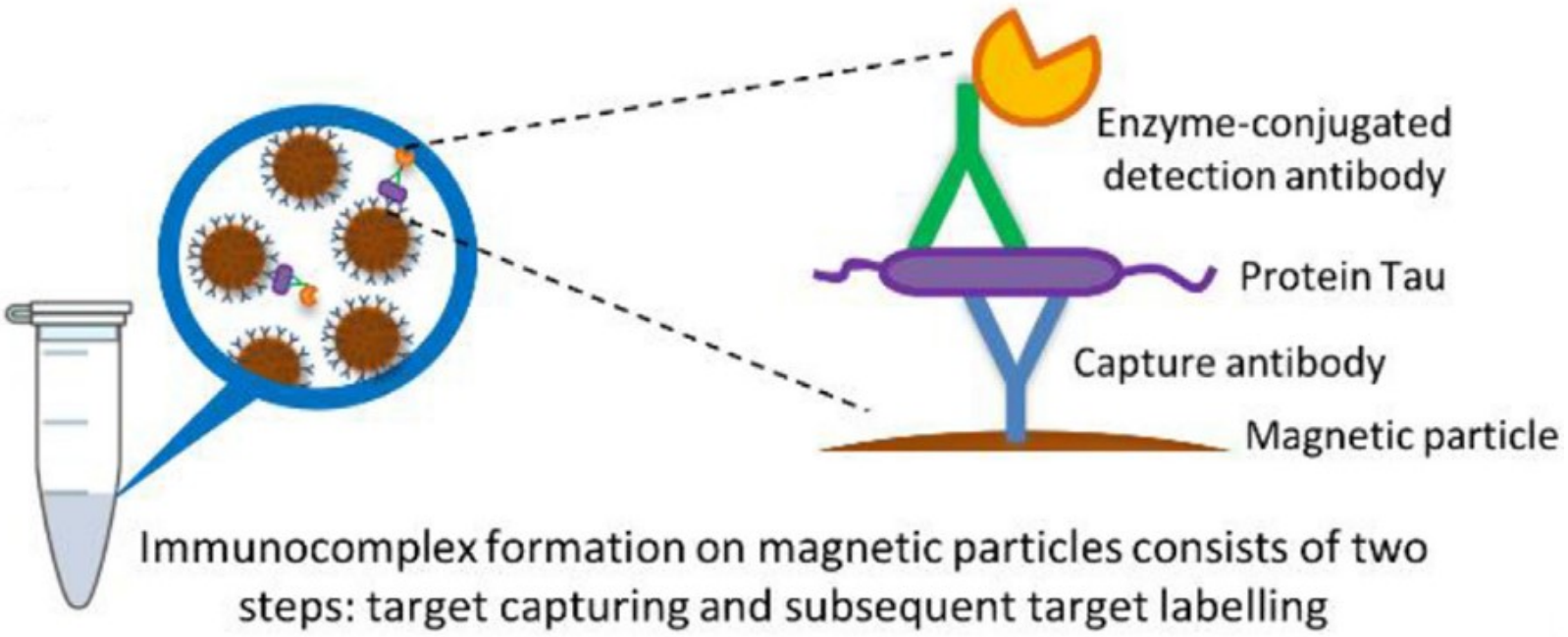


- Magnetic beads used for specific capture of target analyte and reaction with detection antibody conjugated with an enzyme.

EUROPEAN UNION
European Structural and Investment Funds
Operational Programme Research,
Development and Education

MINISTRY OF EDUCATION, YOUTH AND SPORTS

FZU Institute of Physics of the Czech Academy of Sciences

AIT AUSTRIAN INSTITUTE OF TECHNOLOGY

# Digital ELISA

https://doi.org/10.1016/j.aca.2018.02.011

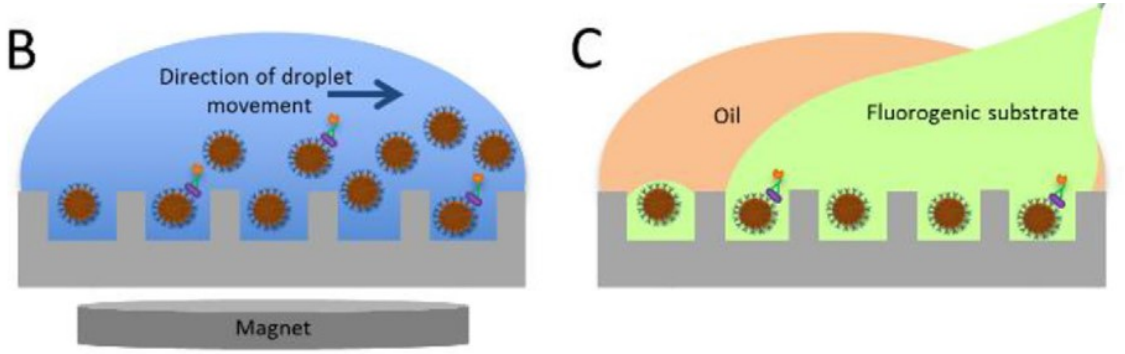


Magnet-assisted seeding of individual magnetic particles in the microwell array

Sealing with oil and formation of femtoliter droplets of the substrate

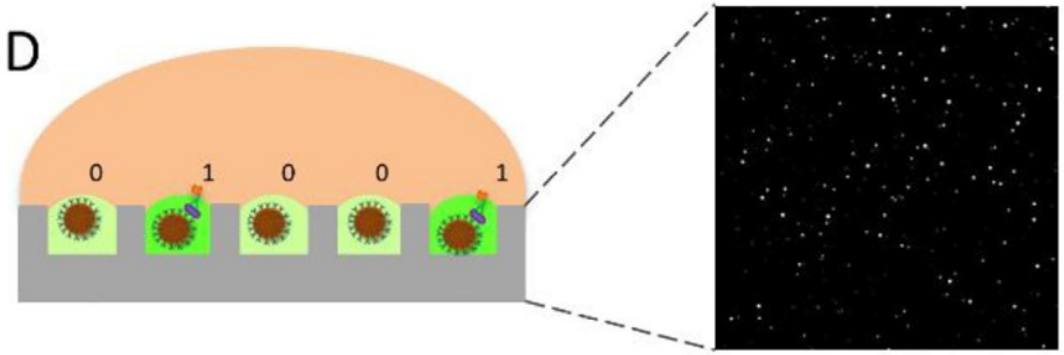


Incubating with fluorogenic substrate until generation of the fluorescent signal (left) and digital counting of single target protein molecules (right)

EUROPEAN UNION
European Structural and Investment Funds
Operational Programme Research,
Development and Education

MINISTRY OF EDUCATION, YOUTH AND SPORTS

FZU Institute of Physics of the Czech Academy of Sciences

AIT AUSTRIAN INSTITUTE OF TECHNOLOGY

# Digital ELISA

https://doi.org/10.1016/j.aca.2018.02.011

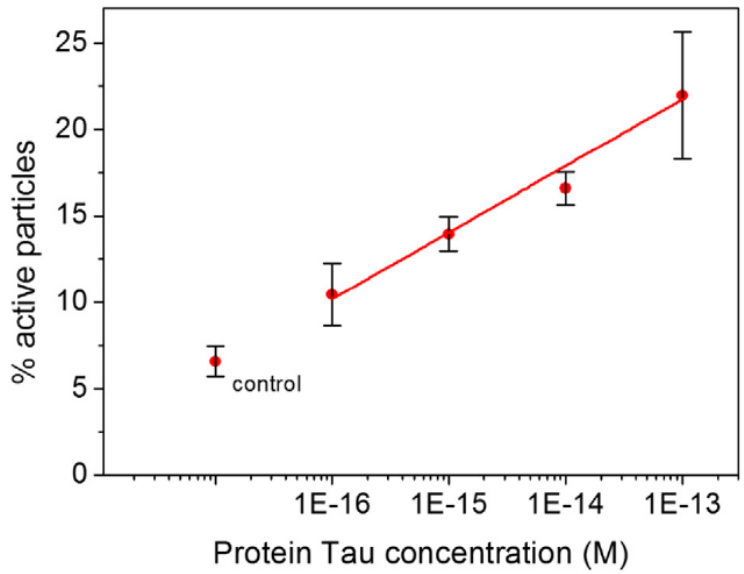


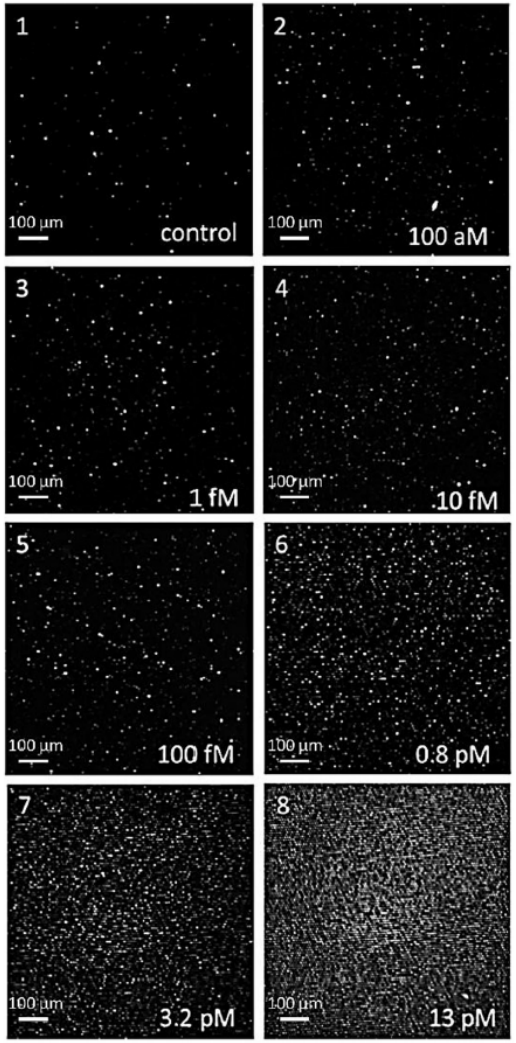


- Tau levels in spiked blood plasma. A similar LOD (55 ± 29 aM) was obtained compared to the buffer samples, which was 5000-fold more sensitive than commercially available ELISAs

EUROPEAN UNION
European Structural and Investment Funds
Operational Programme Research,
Development and Education

MINISTRY OF EDUCATION, YOUTH AND SPORTS

FZU Institute of Physics of the Czech Academy of Sciences

AIT AUSTRIAN INSTITUTE OF TECHNOLOGY

# Commercial Implementation

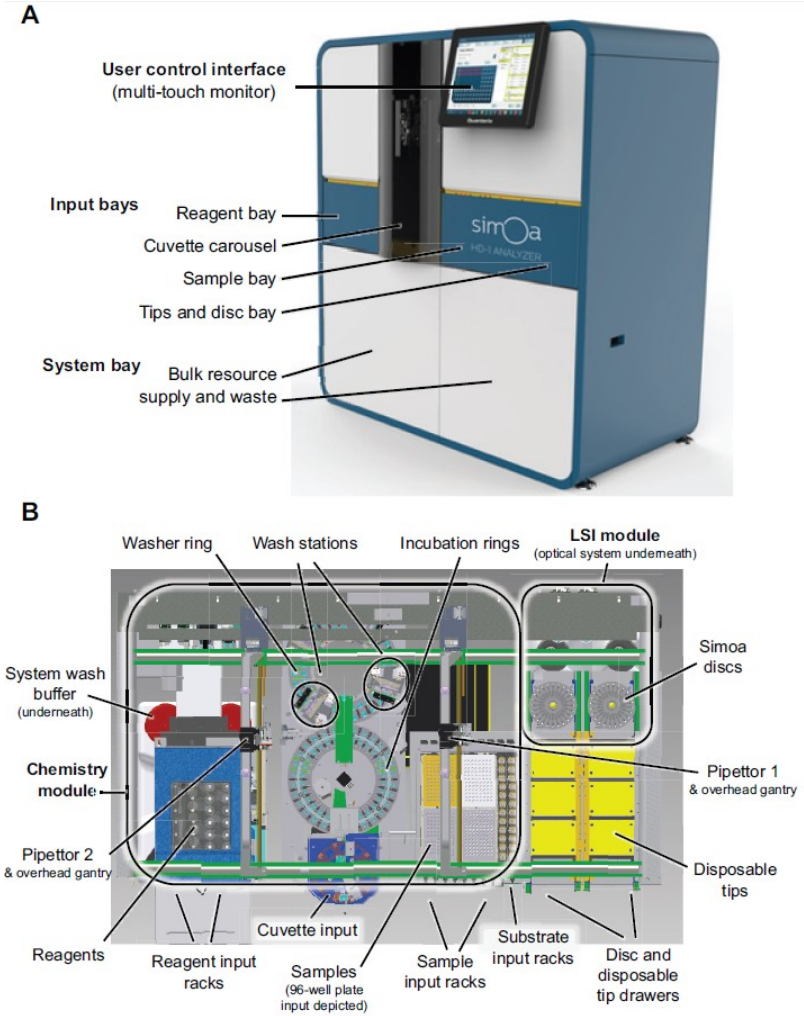


- Digital ELISA was implemented in a commercially available devices by the company Quanterix

DOI: 10.1177/2211068215589580

EUROPEAN UNION
European Structural and Investment Funds
Operational Programme Research,
Development and Education

MINISTRY OF EDUCATION, YOUTH AND SPORTS

FZU Institute of Physics of the Czech Academy of Sciences

AIT AUSTRIAN INSTITUTE OF TECHNOLOGY

# Commercial Implementation

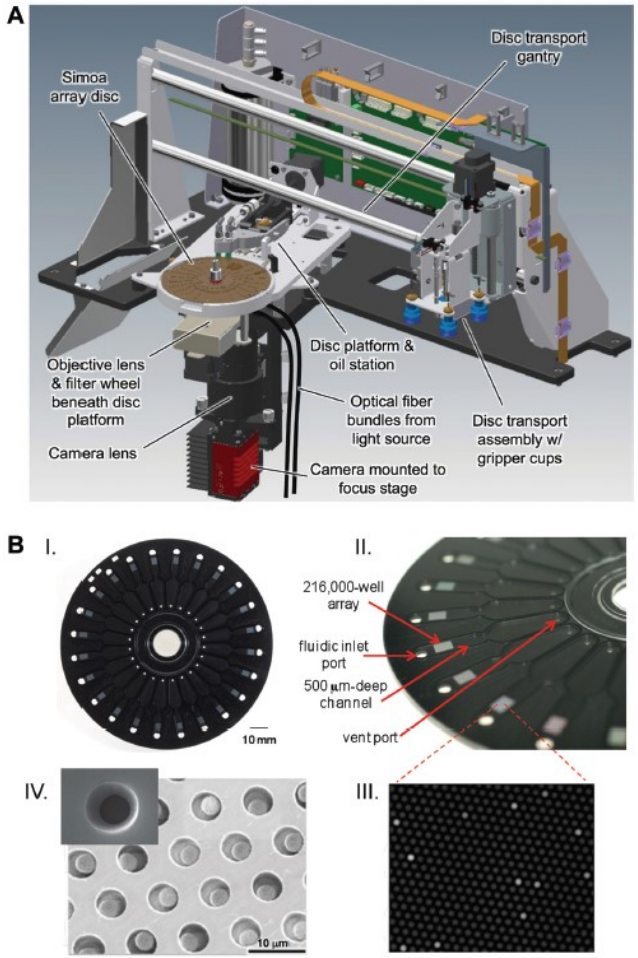


- Implementation of the assay in small compartments and loading of the wells with magnetic beads.
- Fluorescence readout with additional wavelength multiplexing for parallel reaction readout in each well arrays

DOI: 10.1177/2211068215589580

# Commercial Implementation

**Table 1.** Summary of Simoa HD-1 Immunoassay Characteristics.

| Plex | Assay | Sample Volume, µL | Upper Range, pg/mL | Time-to-First-Result, min | Sample | Mean, pg/mL | Within-Run CV, % | Between-Run CV, % | Between-Day CV, % | LoD, pg/mL | LoQ, pg/mL |
|---|---|---|---|---|---|---|---|---|---|---|---|
| 1-Plex | PSA | 25 | 400 | 62 | Low | 3.04 | 6.6 | 8.8 | 0.0 | 0.020 | 0.037 |
| | | | | | High | 60.2 | 5.0 | 4.1 | 6.9 | | |
| | Aβ42 | 25 | 400 | 77 | Low | 2.37 | 3.9 | 10.7 | 3.8 | 0.034 | ND |
| | | | | | High | 51.8 | 5.7 | 6.7 | 2.3 | | |
| | Tau | 38 | 400 | 77 | Low | 2.28 | 6.0 | 14.0 | 0.0 | 0.019 | 0.023 |
| | | | | | High | 109 | 3.8 | 9.1 | 0.0 | | |
| | TNFα | 25 | 200 | 77 | Low | 2.77 | 3.4 | 4.1 | 0.0 | 0.014 | ND |
| | | | | | High | 29.9 | 2.8 | 4.8 | 0.0 | | |
| | IL-2 | 42 | 400 | 62 | Low | 0.589 | 9.3 | 7.8 | 2.2 | 0.011 | 0.100 |
| | | | | | High | 53.7 | 8.8 | 9.2 | 5.6 | | |
| | IL-6 | 25 | 120 | 62 | Low | 1.54 | 5.8 | 0.0 | 2.7 | 0.0020 | 0.0031 |
| | | | | | High | 24.0 | 6.1 | 6.0 | 0.0 | | |
| | IL-8 | 25 | 1200 | 62 | Low | 14.5 | 3.8 | 5.3 | 0.0 | 0.0560 | 0.0921 |
| | | | | | High | 232 | 4.7 | 5.2 | 4.1 | | |
| | IL-10 | 25 | 120 | 62 | Low | 1.68 | 3.5 | 8.2 | 0.0 | 0.0059 | 0.0047 |
| | | | | | High | 29.1 | 5.3 | 5.7 | 4.4 | | |
| | IL-13 | 25 | 300 | 62 | Low | 4.94 | 5.8 | 8.0 | 1.3 | 0.0031 | 0.0114 |
| | | | | | High | 48.1 | 6.0 | 3.2 | 3.9 | | |
| | IL-15 | 25 | 40 | 62 | Low | 0.346 | 4.6 | 4.0 | 0.0 | 0.0030 | 0.0062 |
| | | | | | High | 5.79 | 4.9 | 7.1 | 2.0 | | |
| | IL-17A | 25 | 120 | 62 | Low | 0.505 | 4.4 | 4.0 | 0.0 | 0.0055 | 0.0041 |
| | | | | | High | 26.1 | 4.2 | 7.4 | 0.0 | | |
| | GM-CSF | 25 | 120 | 62 | Low | 0.198 | 6.1 | 9.6 | 9.1 | 0.0035 | 0.0079 |
| | | | | | High | 26.2 | 5.0 | 8.8 | 0.7 | | |
| | IFNα | 85 | 17 | 62 | Low | 0.056 | 9.0 | 7.2 | 0.0 | 0.0014 | 0.0031 |
| | | | | | High | 3.03 | 6.8 | 11.2 | 4.4 | | |
| | C-Peptide | 25 | 400 | 77 | Low | 1.80 | 8.2 | 0.0 | 2.9 | 0.0130 | 0.0210 |
| | | | | | High | 57.2 | 5.4 | 6.0 | 0.0 | | |
| | p24 | 144 | 30 | 62 | Low | 0.088 | 3.4 | 2.3 | 1.1 | 0.0025 | 0.0076 |
| | | | | | High | 8.92 | 5.3 | 3.8 | 1.6 | | |
| | Troponin I | 42 | 1200 | 45 | Low | 2.55 | 7.6 | 5.1 | 7.2 | 0.010 | 0.079 |
| | | | | | High | 115 | 5.4 | 8.1 | 9.7 | | |
| 3-Plex | TNFα | 25 | 120 | 77 | Low | 1.80 | 5.7 | 3.7 | 6.2 | 0.0120 | 0.0505 |
| | | | | | High | 43.3 | 7.9 | 5.5 | 4.7 | | |
| | IL-6 | | 24 | | Low | 0.966 | 5.0 | 6.0 | 6.4 | 0.0060 | 0.0107 |
| | | | | | High | 23.6 | 7.5 | 6.3 | 5.6 | | |
| | IL-10 | | 60 | | Low | 0.492 | 5.7 | 5.3 | 3.9 | 0.0019 | 0.0073 |
| | | | | | High | 11.4 | 4.6 | 6.8 | 7.2 | | |

MW=21 kDa

corresponding to 0.1 fM

For analyzed 25 µL detected about $10^3$ molecules

DOI: 10.1177/2211068215589580

EUROPEAN UNION
European Structural and Investment Funds
Operational Programme Research,
Development and Education

MINISTRY OF EDUCATION,
YOUTH AND SPORTS

FZU Institute of Physics of the Czech Academy of Sciences

AIT AUSTRIAN INSTITUTE OF TECHNOLOGY

# Quanterix Application Fields

Oncology

Neurology

Cardiology

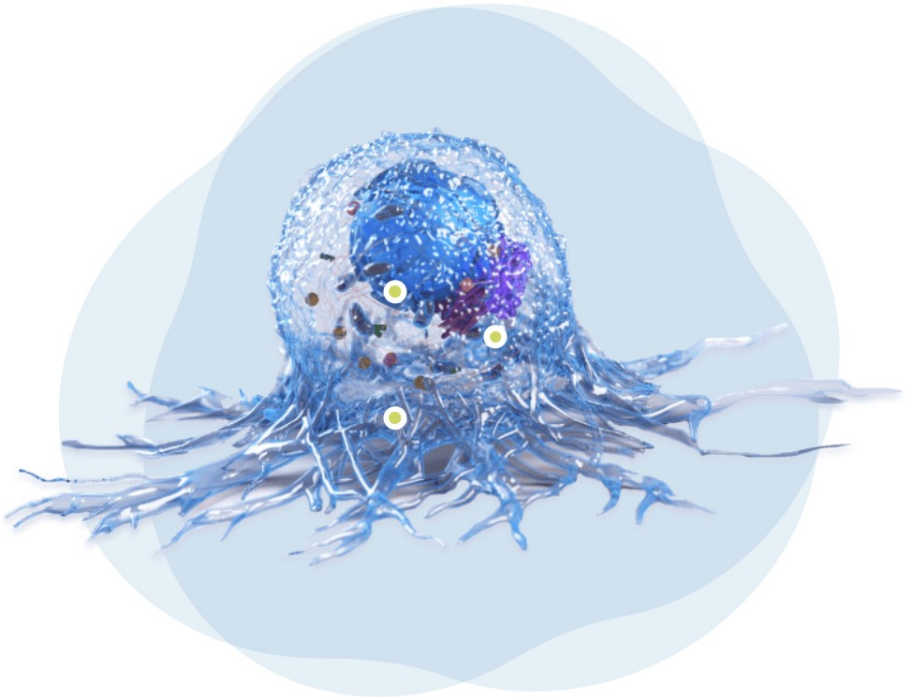

Immunology/
Inflammation

Infectious
Disease

DOI: 10.1177/2211068215589580

# Nanoswitch ELISA (NLISA)

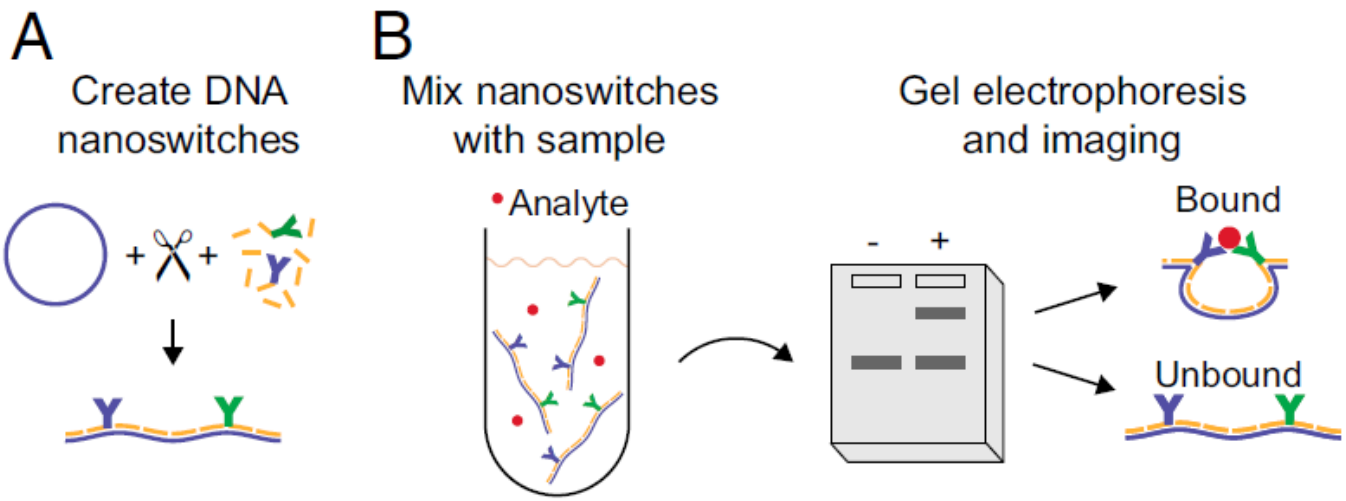


**Fig. 1.** Schematic of the DNA nanoswitch detection technique. (*A*) DNA nanoswitches are created by hybridizing antibody–oligonucleotide conjugates and tiling oligonucleotides onto a linearized M13 scaffold. (*B*) DNA nanoswitches can be stored at 4 °C, and then an aliquot can be added to the sample. The resulting mixture is run on an agarose gel and imaged, with positive signal given by the intensity of the slower migrating band that corresponds to looped nanoswitches that have analyte bound.

www.pnas.org/cgi/doi/10.1073/pnas.1708148114

EUROPEAN UNION
European Structural and Investment Funds
Operational Programme Research,
Development and Education

MINISTRY OF EDUCATION, YOUTH AND SPORTS

FZU Institute of Physics of the Czech Academy of Sciences

AIT AUSTRIAN INSTITUTE OF TECHNOLOGY

# Nanoswitch ELISA (NLISA)

www.pnas.org/cgi/doi/10.1073/pnas.1708148114

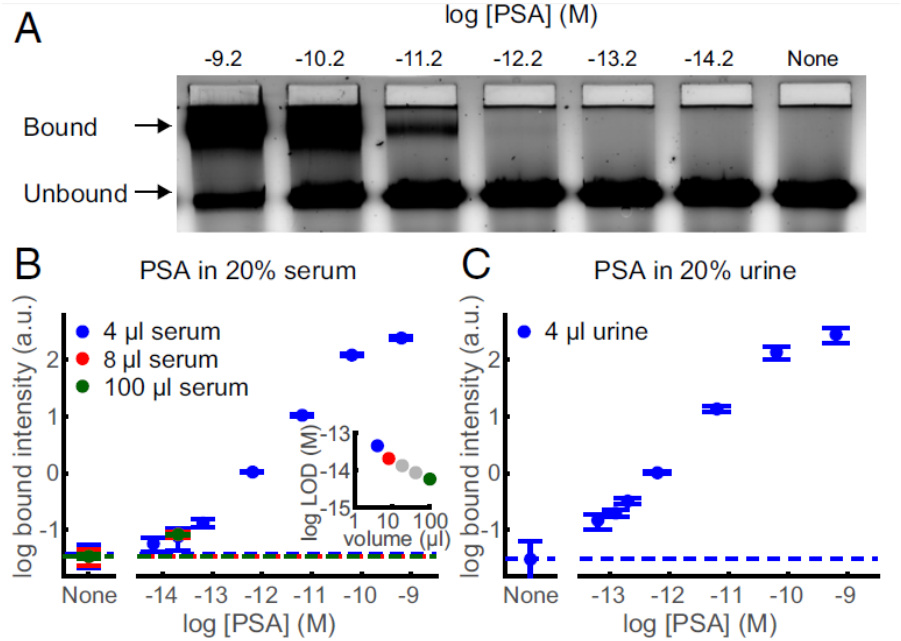


**Fig. 3.** DNA nanoswitch detection of human prostate-specific antigen (PSA) in complex fluids. (*A*) Representative gel image of human PSA spiked into 20% FBS, with concentrations ranging from $6 \times 10^{-15}$ to $6 \times 10^{-10}$ M and a control lane lacking any PSA. (*B* and *C*) Log-log plots of average bound intensity per lane as a function of concentration for PSA in (*B*) 20% serum or (*C*) 20% urine. Results are for 4 µL of serum or urine (i.e., 20 µL of diluted sample) run in one gel lane (blue), 8 µL of serum run across two gel lanes, or 100 µL of serum run across multiple gel lanes. (*B*, *Inset*) Limit of detection (LOD) as a function of sample volume. LOD was determined by extrapolating the concentration from the signal equal to background signal plus 3 SD of the background signal. Error bars are the SD, with the background given by the dashed line, with four replicates per data point, except for None, which has 20 replicates.

EUROPEAN UNION
European Structural and Investment Funds
Operational Programme Research,
Development and Education

MINISTRY OF EDUCATION, YOUTH AND SPORTS

FZU Institute of Physics of the Czech Academy of Sciences

AIT AUSTRIAN INSTITUTE OF TECHNOLOGY

# Two Photon-Fluorescence

10.1021/acs.analchem.7b03542

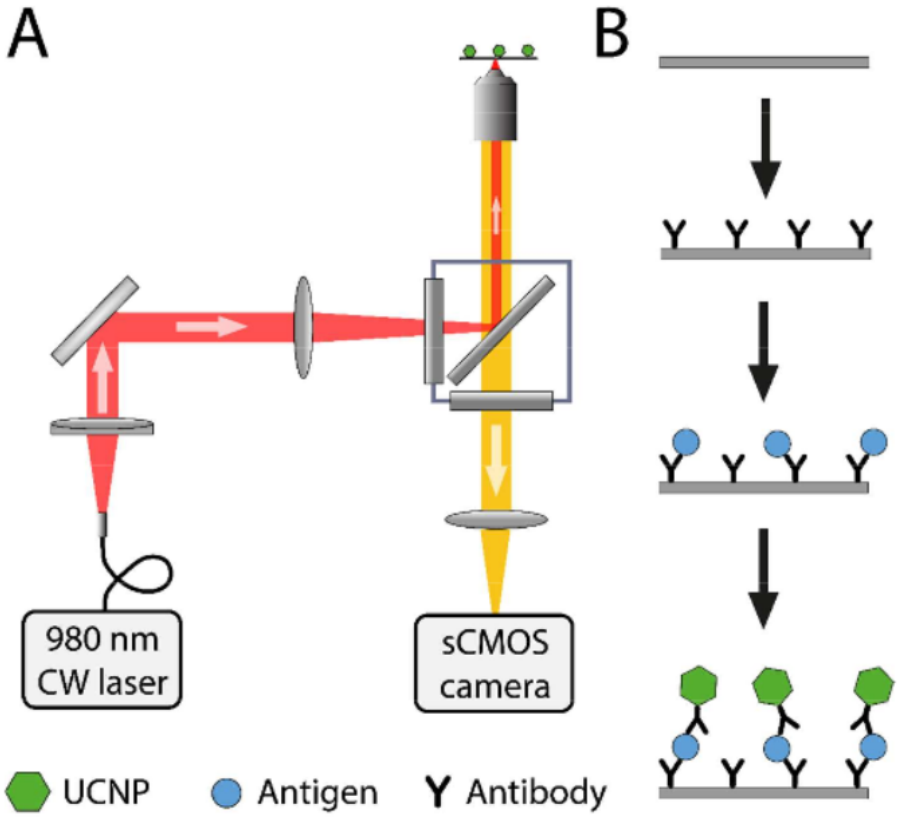


**Figure 1:** A) Scheme of upconversion microscopy. An inverted wide-field epiluminescence microscope is equipped with a fiber-coupled 980 nm continuous-wave laser diode and a sensitive sCMOS camera. B) Scheme of sandwich upconversion-linked immunosorbent assay (ULISA) involving (1) immobilization of the anti-PSA capture antibody, (2) binding of the analyte PSA and (3) analyte detection by a UCNP-antibody conjugate.

EUROPEAN UNION
European Structural and Investment Funds
Operational Programme Research,
Development and Education

MINISTRY OF EDUCATION, YOUTH AND SPORTS

FZU Institute of Physics of the Czech Academy of Sciences

AIT AUSTRIAN INSTITUTE OF TECHNOLOGY

# Two Photon-Fluorescence

10.1021/acs.analchem.7b03542

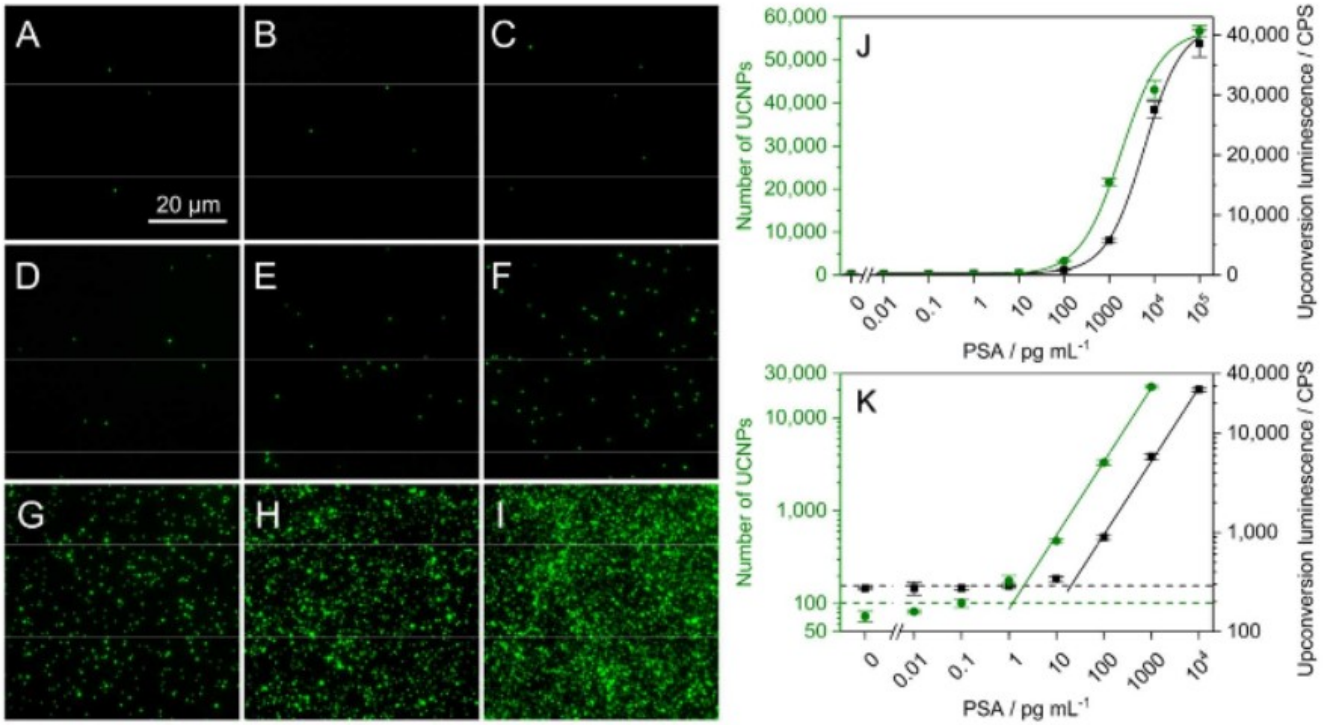


**Figure 4:** Upconversion microscopy images of serial PSA dilutions in 25 % serum: A) no PSA; B) 10 fg $mL^{-1}$; C) 100 fg $mL^{-1}$; D) 1 pg $mL^{-1}$; E) 10 pg $mL^{-1}$; F) 100 pg $mL^{-1}$; G) 1 ng $mL^{-1}$; H) 10 ng $mL^{-1}$; I) 100 ng $mL^{-1}$. PSA is captured on microtiter plate wells and detected by a UCNP-antibody conjugate. A small section (3 600 $\mu m^2$) of the analyzed area (210 × 263 $\mu m^2$) is shown. J) Calibration based on a 4-parameter logistic regression model shows a test midpoint ($EC_{50}$) of 1.8 ng $mL^{-1}$ for the digital readout (green line) and 5.9 ng $mL^{-1}$ for the analog readout (black line). K) Linear regression after logit transformation yields an LOD of 1.2 pg $mL^{-1}$ in the digital readout and 20.3 pg $mL^{-1}$ in the analog readout. The hatched lines are the background level defined either as mean number of spots (green) or upconversion luminescence (black) without PSA + 3× standard deviation. Error bars indicate the standard deviation from three replicate wells.